PERFORMANCE OF POLYMER COATINGS UNDER FORMING CONDITIONS

A Thesis

by

ZALAK PUROHIT

Submitted to the Office of Graduate Studies of
Texas A&M University
in partial fulfillment of the requirements for the degree of

MASTER OF SCIENCE

December 2010

Major Subject: Mechanical Engineering

PERFORMANCE OF POLYMER COATINGS UNDER FORMING CONDITIONS

A Thesis

by

ZALAK PUROHIT

Submitted to the Office of Graduate Studies of
Texas A&M University
in partial fulfillment of the requirements for the degree of

MASTER OF SCIENCE

Approved by:

Chair of Committee,	Jyhwen Wang
Committee Members,	Cris Schwartz
	Wei Zhan
Head of Department,	Dennis L. O'Neal

December 2010

Major Subject: Mechanical Engineering

ABSTRACT

Performance of Polymer Coatings Under Forming Conditions. (December 2010)

Zalak Purohit, B.E., Osmania University

Chair of Advisory Committee: Dr. Jyhwen Wang

Prepainted metal sheets being environment friendly and cost effective as compared to postpainted metal sheets, are widely used in construction, packaging, transportation and automotive industries. One of the key requirements for prepainted coatings is to retain its surface quality and properties during forming process. During forming process, major surface damage occurs when the coated sheet is bent and un-bent around the die corner. To reduce surface damage of coatings, proper control of the parameters during forming and detail study of the surface conditions is required.

In the present study, influence of forming parameters such as die radius, lubrication and specimen material are investigated. The influence of these parameters on friction, surface damage and properties of polymer coatings are evaluated. Experiment set-up is built to conduct bending under tension test. This test gives a better way to evaluate coating performance, as it closely simulates the die region of real forming process and considers bending effects.

Experimental results show increase in friction and surface damage with decrease in die radius. Moreover, with decrease in die radius hardness of the coating decreases and strain in the specimen increases. Lubrication has some effect on coefficient of friction, but the influence is not as significant as that of die radius. This is attributed to the fact that, the polymer coating itself acts as a solid lubricant in the test. Material effect was studied, polypropylene coating being the softer material compared to PVDF coating shows more surface damage in the form of scratches.

Numerical simulations were performed using Finite Element Analysis package (FEA) Abaqus. A 2D model was built, exploiting the plane strain condition for bending under tension test. Numerical simulations indicate that maximum contact pressure and von Mises stress are concentrated at the beginning of the drawing edge. Apart from the location, the value of contact pressure was higher for smaller die radius.

Thus, experiments help in studying the effect of forming parameters on coating performance and numerical simulations provide more insight into the critical areas where stresses are high. Numerical simulations also provide a scope to study the effect of material and geometirc parameters on performance of coatings without running experiments.

ACKNOWLEDGMENTS

Firstly, I am very grateful to my advisor Dr. Jyhwen Wang for giving me an opportunity to work under him on this project. He always guided me through my project and patiently answered my questions. He also motivated me to learn and try new ideas in my thesis. I am thankful to Dr. Wei Zhan for being on my thesis committee and help me with instrumentation and electronics part of my experiment. I would like to thank Dr. Cris Schwartz for his valuable inputs through the tribology course and consenting to be my committee member.

I wish to offer special thanks to Mr. Robert Barber and Mr. Charlie Mobley for their invaluable help while setting up the experiment set-up. I am also grateful to Dr. Wayne Hung and Mr. Adam Farmer for allowing and guiding me to use the instruments for material characterization. I am indebted to Bright Wadja and Sunku Bhanu for their help while conducting experiments. I also thank all my other friends and roommates for their support and help all through my project.

Most importantly, I am very thankful to my parents Gopal and Arati Purohit for their love, support and encouragement. This would not have been possible without their help and sacrifices.

TABLE OF CONTENTS

CHAPTER Page

CHAPTER Page

LIST OF TABLES

TABLE Page

LIST OF FIGURES

FIGURE Page

CHAPTER I

INTRODUCTION

Metals sheets are widely used in major industries because of their high ductility and varied range of mechanical strengths compared to other materials like ceramics and polymers. Surface of these sheets is painted with different paint systems which provide glossy decorative surface finish and protection against corrosion. These painted metal sheets are widely used in automotive, construction, transportation, consumer products and packaging industry.

Although coating the surface has many advantages, the organic compounds (VOC) present in paint system disperse and evaporate in the atmosphere during curing which are hazardous to environment and health. These emissions can be reduced, if post-painting of the metal sheets is avoided.

A. Pre-painted Metal Sheets

To avoid painting of metal sheets after forming, pre-painted metal sheets were introduced. Permanent coating is first applied on metal sheets followed by a forming process to obtain a desired shape.

1. Coating Methods

Various technological methods have been used to coat the surface of metal sheets ensuring uniformity and quality performance of the polymer coatings. Coil coating is one of the commonly used coating techniques in industries. It is automatic and continuous process which coats very large sheets on both top and bottom in one single

---

The journal model is *IEEE Transactions on Automatic Control.*

process.

In coil coating process, metal sheets are first cleaned to provide a clean surface. This is followed by a pretreatment on surface of the sheet by chemicals. Chemical treatment ensures bonding between steel surface and subsequently applied paint. In the next step, primer is applied on coating surface to provide flexibility and corrosion resistance by corrosion inhibitors present in the primer. Primer is then cured as the material passes through the curing oven at carefully controlled temperature.

Finally, a top coat is applied on the primer and is again passed through the oven for curing. The direction of the rotation of the applicator roll plays a major role in applying a particular type of coating. When the roller rotates in opposite direction to the sheet, it is called reverse roller coating and is used for thick coatings. When the rotation is in the same direction as the sheet, it is called as direct roller coating, used for thinner coatings.

Prepainted coils can also be embossed, printed and textured using coil coating method [1]. Spin coating, physical vapor deposition and chemical vapor deposition are some other types of coating methods. These are generally used to obtain very thin and precise coating thickness.

2. Advantages

Pre-painted metal sheets offer various advantages over post-painted metal sheets. Besides reducing harmful emissions, they enhance productivity, reduce processing cost and provide better quality products. The other unique advantages offered by them are:

1. Corrosion protection to metallic sheets and better resistance against harsh weather.

2. They act as dry lubricants in the forming process. This eliminates the need of using lubricants and improves the formability of metal sheets.

3. They eliminate the need for wash/coat/spray and are free of uneven application or defects on the surface due to the same. They are also free from dirt or any other residuals on the surface.

4. As they eliminate VOC emissions (there is no curing process), pre-painted polymer sheets are eco-friendly.

5. Forming of polymer sheets is less time consuming and an energy efficient process. They have less transportation, storage and production cost and is more energy efficient when compared to the conventional spraying methods.

6. Pre-painted polymer coat provides glossy and aesthetic finish to the surface.

3. Polymer Properties

Polymers exhibit covalent bonding within chains and secondary bonding (Vander Walls bonding) between each layer. They are thermally and electrically insulated. They have low density and high resistance to chemical reactions. They are mechanically weaker than metals. Polymers have low elastic moduli and are very easily moldable.

Mechanical properties of the polymers are sensitive to temperature and the strain rate. On increasing the temperature and decreasing the strain rate, the material becomes more softer and ductile. At glass transition temperature, polymer changes from a rigid state (at low temperature) to a rubbery state (at intermediate temperature). At intermediate temperatures, they exhibit viscoelastic property. For viscoelastic behavior of polymers, they exhibit viscous, time dependent strain behavior [2].

Many additives are added to improve the properties of polymers. Wax is added to improve lubrication, and ceramic fillers to improve the mechanical properties. These advantages and properties of polymers make it an ideal choice to be used as a coating on metal sheets. Polymer coatings are used in many applications such as for car components, building roofs, beverage cans, packing materials etc.

4. Components of Coating System

A polymer coating system consists of a primer and a top coat. The important functions of a primer involve wetting the substrate surface, acting as an adhesive, and providing corrosion resistance. The top coat has a glossy finish and provides UV light protection. Pigments, binders and solvents are major components of the paint system. The pigments provide corrosion inhibition, binders link the substrate to the top coat and solvents disperse the binder and allow the coating to spread out [3]. The thickness of these coatings range from scale of nanometers to micrometers.

B. Forming of Pre-painted Metal Sheet

The sheet metal forming process consists of cutting operations or operations involving plastic deformation. Bending, stretch forming and deep drawing are some of the examples of a plastic deformation process. This process involves a change in the shape of work-piece (as desired) without any cutting operation. Performance of the process depends on properties of sheet metal, die geometry and forming conditions.

In bending, a uniform sheet is linearly strained along an axis lying in the neutral plane and perpendicular to the length of the sheet. Different bending operations are V-bending, U-bending, roll bending, edge bending etc. In stretch forming, the edges of the sheet metal are clamped and the sheet is pulled with the help of a die or a

block. Movement and geometry of die depends on the shape of the final product desired.

Deep drawing process is a compression-tension forming process involving wide spectrum of operations and flow conditions. In this process, blank is pulled over the punch into the die. The blank holder clamps the metal sheet by applying force. It allows the sheet to flow between blank holder and the die unlike stretch forming to avoid wrinkling. A flat sheet is formed into a cup shape with minimum number of operations and scrap using deep drawing process as shown in Fig. 1.

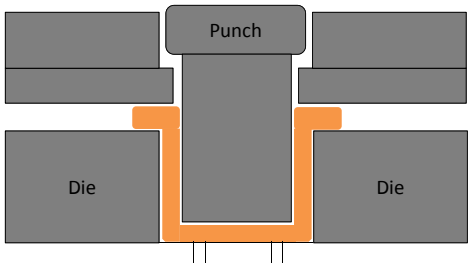

Fig. 1. Deep Drawing Process [4]

Deep drawing process has the capability of producing high strength final products and complex geometries which are difficult to achieve by other forming processes. The performance of this process depends upon the die geometry, die surface, material properties, blank holder force, punch velocity, strain hardening and strain rate.

In spite of numerous advantages offered by polymer sheets, one of the key requirements is to survive the manufacturing process which converts it into the final product. Coating should not be deformed during operations like cutting, bending, stamping or deep drawing process. The coating should be flexible, strong, have high formability and should also maintain its hardness after forming.

C. Defects in Coatings During Forming

During forming, coating has to be free from defects like scratches, cracks, chipping and peeling. Thus, it is important to know the types of defects and causes for defects. Surface wear and delamination are the two major defects observed, as shown in Fig. 2. The material is removed from the surface of the coat when in contact with sharp edges or corners. This forms scratches or mars on the surface, leading to surface damage of polymer coatings.

Poor adhesion and discontinuity between the top coat and the substrate leads to delamination. These defects cause loss of the attractive and protective properties of the product and should be prevented. The present work concentrates on surface damage during forming.

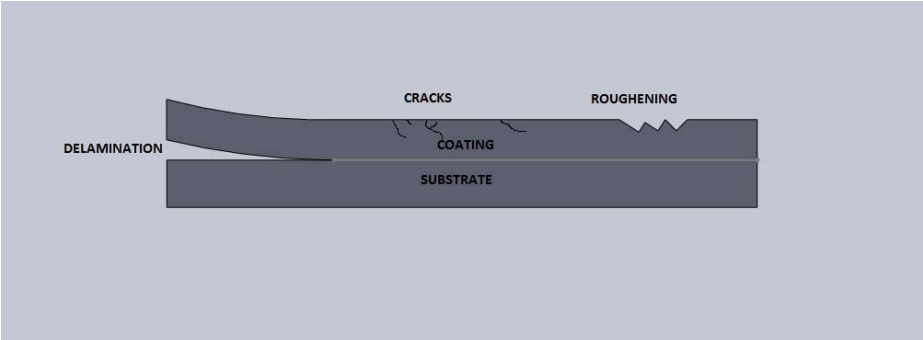

Fig. 2. Defects in Coating [5]

D. Surface Damage During Forming

Surface damage of the polymer coating can be observed during forming of pre-painted sheets. Damage in the form of scratches and loss of glossiness on the surface of the coatings is seen. Major surface damage occurs when the coated sheet is bent and

un-bent around the die corner. The proper control of parameters during forming and detailed study of the surface wear can reduce the surface damage of coatings.

1. Surface Wear

Surface wear is defined as the gradual loss of material from the surface of one body due to sliding interaction with another body. In sheet metal forming, wear takes place by different mechanisms leaving behind scratches on the surface of final product. According to Schuler, wear can be classified into five basic ways [6]. They are deformation, wear at surface layer, adhesion wear, abrasive wear and fatigue wear. Wear mechanisms have different depth effects on the material which is shown in Fig. 3

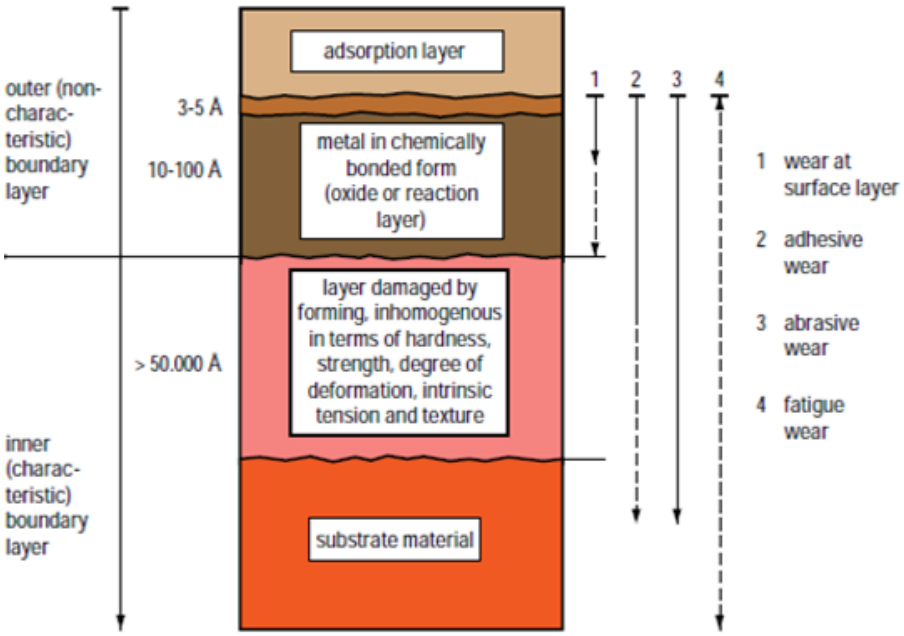

Fig. 3. Types of Wear [7]

Wear at surface layer is also called as tribo chemical wear mechanism. Due to thermal and mechanical processes occurring at the interface, it forms an interfacial

layer between the sliding pair in the form of oxide or reaction layers. These layers have both positive and negative effects. The shear strength of these layers is much smaller than that of the bulk metal, therefore it deforms easily under frictional stress. However, it acts as a protective layer for the substrate underneath under small loading.

Adhesive wear is caused by adhesion of the material to the counter face under sliding. During a forming process the plastic deformation occurs at the asperities causing the lower hardness material to weld to the counter face having higher hardness value [8]. By selecting the sliding pair having different chemical compositions and similar mechanical properties reduce adhesive wear. It can also be minimized by better surface finish and use of lubricants.

The lowest wear is seen in the case of metallic and non- metallic counter faces with similar hardness. Non-metallic coatings on metal substrate show high resistance to adhesive wear and corrosive wear. Thin polymer coatings are generally applied on the metal substrates to reduce galling tendency when sliding against metal counter face.

Abrasive wear is caused by harder irregularities causing cutting or ploughing on the softer counterpart. This wear results in scratches on softer surface. This is generally seen as secondary wear mechanism occurring after adhesive wear where the adhesive particles sticking on to the surface abrades the counter face.

Ploughing component of friction is responsible for abrasion wear. Abrasion wear depends on the relative hardness of the frictional pair in contact. Fatigue wear causes surface failure due to repetitive stress from the hard irregularities on the counterpart. It is generally seen as long term wear.

Surface wear in metal forming is related to friction conditions during the process [6]. Very high Coefficient of friction (COF) will lead to wear on the surface of the sheet which is undesirable and friction is responsible for the stress-strain distribution

in the material during the forming process. Thus, study of friction at the interface of die and sheet metal during forming will give a better understanding of surface behavior.

2. Friction

Friction is the resisting force for relative motion between the two bodies. The phenomenon of friction was first introduced by Leonardo Da Vinci. Further, extensive studies were conducted by Amontons and Coulomb in 1699 and 1785 which gave rise to three fundamental laws of friction. They are:

Law 1: Frictional force is directly proportional to the applied normal force given by equation

$$F = \mu N \tag{1.1}$$

where F= frictional force, N= normal force or load applied and μ= Coefficient of friction.

Law 2: Friction force is independent of apparent area of contact.

Law 3: Friction force is independent of sliding speed.

These laws form basis for the concept of friction and study of friction in sheet metal forming. However, friction in sheet metal forming also depends on many other factors. According to Bowden and Tabor in 1950, friction depends on the true contact area between the surfaces which is very small when compared to apparent contact area [8]. True contact area is formed by the interaction between their asperities and this asperity interaction increases with increase in normal load. An increase in asperity interactions causes more adhesion and influences the frictional force. Besides adhesion, the asperity of one surface ploughs into the other which again causes change in the frictional force. Adhesion and ploughing are two major components of the

frictional force [9].

Coefficient of friction plays a very important role in sheet metal forming operations. As friction is a system parameter, not a material parameter, its value is different for different operations [10]. In most of the operations very low COF is desired for smooth and easy movement but in some operations like deep drawing process, sufficiently high COF is desired to allow the plastic flow of the material and to ensure proper gripping. Very high COF will lead to wear on the surface of the sheet which is undesirable and friction is responsible for the stress-strain distribution in the material during the forming process. Thus, it is very important to control the friction value in a system.

In sheet metal forming, friction depends on various parameters which are not included in the basic laws of friction. The parameters can be divided into three major groups like geometric parameters, process parameters and lubricating systems. Geometric parameters include the die geometry, surface characteristics of the die and of the work piece. Process parameters include the normal force and the sliding velocity. There are different types of lubricating systems used which affects the COF.

Control of these three major parameters will give very smooth surface finish on the final product without any trace of surface wear. Apart from studying the surface finish and friction, study of changes in the properties of coatings is also important. There has been a lot of work done in this field which will be discussed in detail in the next chapter.

CHAPTER II

LITERATURE REVIEW

As seen from the previous chapter, the surface damage depends on various parameters. Study of those parameters will give a better understanding of the causes and reason for surface damage. Various studies relevant to this project have been conducted in the past and can be divided into two major groups; study on bare metal sheets and study on polymer coated metal sheets. Study on bare/metallic coated metal sheets was to characterize the surface damage and friction under forming conditions. Whereas study of polymer coated sheets was mostly related to surface damage and properties of coatings under loads normal to its surface. The present work aims at extending the study on polymer coated metal sheets by performing test under forming conditions (bending under tension loading condition) with the help of knowledge on bare metal sheets. These topics will be reviewed in detail.

A. Study of Surface Damage and Friction on Bare/Metallic Coated Metal Sheets

The major deformation during the forming process occurs when sheet passes through the die region. Different test set-up were built in past to simulate the die region of forming process. These test set-ups were used to study friction and surface damage of bare/metallic coated sheet metals. The test must satisfy criteria such as: deformation mode should be similar to that of original deformation, surface topography and same composition of tool as that of die and the test should operate in the same lubrication system as in the real technology.

1. Different Test Methods to Study Friction

Based on different forming process such as stretch forming, deep drawing and stretch drawing, different test models were used [11]. Stretch forming used three models pure stretch test, olsen and erichsen cup test and strip stretching test. In pure stretch test, the sheet is totally clamped and deformed by a punch. In strip stretching test, the strip is stretched over the radius edge of the tool with constant velocity from one end and other end remains fixed. From the measured extension, coefficient of friction(COF) is measured with an advantage that the actual large deformation occurs in contact zone.

To simulate deep drawing process, swift cup test, bending under tension test (radial deep drawing test), flat die simulator and strip deep drawing tests were commonly used. In swift cup test, blank is drawn to the maximum punch load which occurs before cup is fully drawn. Bending under tension as shown in Fig. 4 aims to simulate material deformation in die radius zone, by drawing the strip over a pin and applying back tension. From measured forces, coefficient of friction is calculated. Flat die simulator is the simplest test, where sheet is drawn between two flat dies. In strip drawing test as shown in Fig. 5, the strip is passed over a flat die and bent over die radius zone [12].

Bending under tension test and strip deep drawing test has advantages over swift cup and flat die simulator test. Swift cup test does not concentrate on individual complex zones and flat die simulator does not correlate well to the real process. Bending under tension test and strip deep drawing test correlates very well to the real process and concentrates on individual complex zones. The other method, stretch drawing involves both stretch forming and deep drawing. This employs draw bead simulator. For adequate amount of force to bend and unbend the strip, draw beads

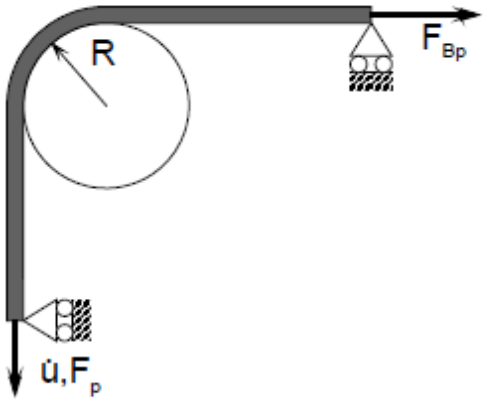

Fig. 4. Bending under Tension Test [11]

are used.

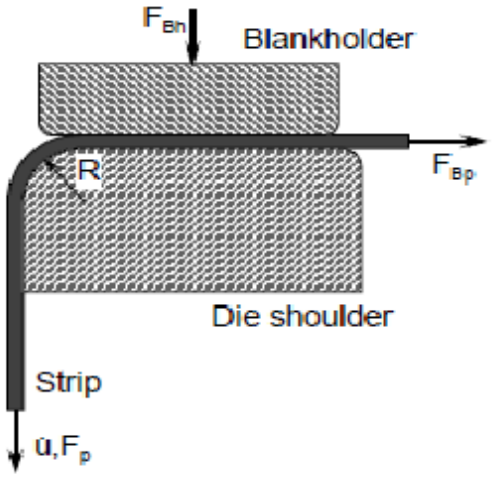

Fig. 5. Strip Deep Drawing Test [11]

2. Development of Friction Models

Bending under tension test method was most commonly used to characterize friction and surface damage. Different approaches were developed in the past to calculate

coefficient of friction (COF) at the die region in bending under tension test. Incremental energy balance, incremental force balance and system force balance were the approaches developed. Using incremental force balance, equation for coefficient of friction was calculated by Swift given in Eq. 2.1 [13]. This equation was modified further to consider the effect due to bending on the forces. The effect of die radius and sheet thickness was also accounted in the equation for COF given in Eq. 2.2 [14].

$$\mu = \frac{1}{\theta} \ln(\frac{f1}{f2}) \tag{2.1}$$

$$\mu = \frac{1}{\theta}(\frac{r + 0.5t}{r}) \ln(\frac{f1 - fb}{f2}) \tag{2.2}$$

Second approach used was incremental energy balance, derived for a bend angle of 90°. This approach, considers the effect of die radius and the sheet thickness as given in Eq. 2.3 [15]. Third approach was developed by Wilson. He used system force balance approach for finding coefficient of friction. This approach neglected the effect of bending force and sheet thickness given by Eq. 2.4 [16].

$$\mu = \frac{2}{\pi}(\frac{r + 0.5t}{r}) \ln(\frac{f1 - fb}{f2}) \tag{2.3}$$

$$\mu = \frac{2}{\theta}(\frac{f1 - f2}{f1 + f2}) \tag{2.4}$$

On comparing the results from these three approaches, the bending contribution in the calculation of friction coefficient was found to be important [10]. In same study, six metallic coated sheets were tested using bending under tension test. Coefficient of friction was calculated by energy balance approach which considers the contribution due to bending. COF was observed to be different for different material types and it was also found to depend on the contact pressure.

3. Experiment on Bare Metal Sheets

Saha conducted friction experiments on uncoated metal sheets using bending under tension test [16]. The experimental set up of Saha consists of two linear actuators which stretches and slides the specimen over a cylindrical pin. Actuators were driven by stepping motors and were equipped with proper grips for specimen and load cells to measure force during forming. The whole set up is controlled by personal computer, three axis stepper motor drive system and A/D converter which measure the load cells and velocity sensors.

The set up allows an independent control of all process variables that affect friction coefficient during forming process. Process variables such as contact pressure can be changed by changing pin radius, sliding velocity and strain rate can be changed by changing motion control parameters and strain in contact can be changed by changing angle of wrap [17]. Saha used system force balance approach developed by Wilson to calculate the COF. As bending effect was observed to be significant; he included bending-unbending force computed by Swift methodology in the equation [13].

The effect of plastic strain on COF was studied. Two sets of experiments were conducted, first set of experiments were conducted with electro-galvanized steel sheets on smooth A2 die steel and second set of experiments with lubricated 1100 H-14 aluminum on smooth cemented carbide. The variation of COF with plastic strain was found to depend on the characteristics of material being formed. The material that has more tendencies to roughen with plastic strain will show decreased COF whereas material that has less tendency to roughen will show high COF.

Bending under tension test set up which is similar to the one used in Saha's experiment but with constant back tension was used. Using this set-up, the effect

of average contact pressure on surface roughness and COF was studied. The specimen used was A1100 aluminum sheet of dimensions 500×10×1mm(L×W×T). The die used is made of tool steel and the paraffin base oil is used as a lubricant. Coefficient of friction is calculated from the forces measured, die angle and the bending force. Surface roughness was measured by contact needle type roughness meter and elongation was measured by using scribed pattern on the specimen [18].

At lower contact pressure, the surface roughness of the inner surface of the specimen was observed to increase with increase in average contact pressure due to surface roughening of the specimen. Whereas at higher contact pressure, the surface roughness of the inner surface was observed to decrease with increase in average contact pressure due to asperity flattening. For lower contact pressure, the COF was constant and for higher contact pressure, the COF decreased with increasing contact pressure. At lower contact pressure, surface roughening dominates and boundary lubrication regime was observed whereas at higher contact pressures, surface flattening dominates and hydrodynamic lubrication regime was observed which was responsible for lowering the COF at higher contact pressure.

Galvanized steel and Galvannealed steel sheets are widely used in automotive industry and they show significant amount of surface damage during the forming process. The surface damage of the Galvanized steel and Galvannealed steel was evaluated and the influence of factors such as tool hardness and the number of forming passes were studied [19]. An experimental simulation of forming process of a U-channel part with draw-bead (draw bead is used to limit the material flow and maintain a constant strain distribution) was carried out to study the surface topography of the Galvanized steels. The contact conditions of sliding under tension and bending was simulated in the experiment.

The Galvanized and Galvannealed sheets used for experiments have same sub-

strates (to nullify the effect of substrate in the study). The hardness of the specimen was measured using micro hardness test and surface roughness using stylus profilometer. The tool material used was Mo-Cr cast iron with three different grades of hardness HRC35, HRC45 and HRC52. It was observed that both Galvanized and Galvannealed steel increases its surface damage by increasing number of forming passes. With increase in hardness of the tool, the surface damage reduces in case of Galvanized steel whereas for Galvannealed steel an optimum hardness of the tool has to be selected to reduce the surface damage. The Galvanized steel shows scratch damage whereas Galvannealed steel depicts ex foliating followed by severe scratching. Galvanized steel acts as lubricant whereas Galvannealed steel is more brittle. All these studies indicated that the formability of Galvanized steel is better than Galvannealed steel.

The other work relevant to friction and surface damage of metal sheets involved building a new set-up to replicate bending under tension test [20]. Test set-up was designed similar to Saha's and Wilson's Sheet metal forming simulator with 90° angle of contact. It had mechanical components to secure specimen and for movement of specimen, load cells to measure forces and data acquisition system to read the load values into a computer. Steel specimens were tested with specimen dimensions of $500\times18\times1\times$ mm.

The influence of parameters such as tool pin radius, tool pin surface finish, specimen material and lubricating conditions were tested. The friction coefficient was calculated using Wilson's model. The bending force was considered in the present friction calculations. Bending force was determined by replacing the tool pin with the bearings of same diameter. When the sheet is rolled over the bearings, the sheet becomes insensitive to friction at the contact region. Thus, bending force can be determined as difference between the front and the back force.

The chrome surface finish on tool pin was compared with machine surface finish

on tool pin. Chrome surface finish was observed to reduce friction coefficient under some cases and increase in other cases. Thus there was no clear influence of surface finish of the tool pin on the friction values. As the chrome finish has lower surface roughness than machine finish, the real contact area of chrome finish is more than machine finish. This can cause more friction coefficient in case of chrome finish than machine finish.

There was no particular trend observed in friction coefficients by changing the pin diameter in the set-up. The effect of grease was very small in reducing friction coefficient. The use of teflon had reduced the friction coefficient by a large value. Use of teflon as a solid lubricant was observed to help in even separation between tool pin surface and the specimen. It provided a very good material flow conditions in a forming process.

4. Numerical Simulations on Bare Metal Sheets

Experimental analysis was extended to numerical simulations. Numerical simulation was employed to find the relation among various parameters used in deep drawing process. Mild steel was used for simulating cup test with thickness of 0.8mm and was assumed to be anisotropic [11]. For different value of clearances keeping coefficient of friction constant and different coefficient of friction keeping clearance constant the test was simulated. A commercial finite element program LS DYNA was used for simulation. The elements used were 4-node Belytschko-Tsay shell elements, which provide five integration points through the thickness of the sheet metal.

It was observed that with the increasing coefficient of friction; axial forces increase (with clearance constant) and with increase in clearance; axial forces decreases (with friction coefficient constant). Similarly the experimental simulation of friction was devised to find the effect of lubrication on axial force with time. It was observed that

initially force increases rapidly and over a time it reduces to constant force value, thus an adequate amount of lubricant is required to keep the force constant. The results from numerical simulation and experimental work were in accordance with each other and were used to find the optimum value of coefficient of friction and lubrication for a deep drawing process.

All the above mentioned experiments and numerical simualtions were all focused on the study of parameters that influence surface damage and friction in uncoated/metallic coated sheet materials under forming conditions.

B. Study on Polymer Material and Polymer Coated Sheet Metals

With wide use of polymers in food packaging, aerospace, automobile, coatings and microelectronic packaging industries, lot of work was done in past to evaluate the properties of polymers and the performance of polymers under various conditions. To study the performance of polymer coated metal sheets, various test were conducted with load normal to the surface of the coatings and the effect of various parameters on its performance was evaluated.

1. Hardness Measurements

Nano and micro indentation techniques as well as micro mar resistance techniques were used to characterize the surface of the films. Many factors were observed to cause effect on the characterization of these films. Substrate effect was observed to be one of the significant factors. The substrate effects the mechanical characterization of surface of the films, if the indentation depth surpasses a critical depth value.

a. Experiments and Factors Influencing the Hardness Measurements

Previous experiments observed that the film hardness depends not only on geometric constraints of substrate, but also on structural constraints, like grain boundaries. To evaluate the structural effect, vickers micro hardness test was conducted on single crystal, polycrystalline and nanostructured multilayer films deposited on various substrates [21].

The coating thickness was measured using optical interferometry technique. Vickers micro hardness test was performed on the specimen and the diagonal length of the residual imprints was measured with a neophot-30 microscope. Hardness was measured for each system as a function of applied load and indentation depth as 1/7 of the impression diagonal length. The critical indentation depth above which the hardness is affected by the substrate is determined and results are analyzed using dimensionless parameters such as indentation depth/thickness of the film and hardness of film/hardness of substrate.

Closer the mechanical properties of coating and substrate, less effect of substrate on critical indentation depth was observed. For soft coatings on hard substrates, the Lawns relation given in Eq. 2.5 [21] was found to be applicable in determining critical indentation depth. In the relation, H is hardness, E is the modulus of elasticity, hc is the critical indentation depth and t is the thickness of the film.

$$\frac{h_c}{t} = 0.42(\frac{H}{E})^{\frac{1}{2}} \tag{2.5}$$

In case of hard coatings on soft substrates, the critical indentation depth was observed to depend on the plastic yielding of the soft substrate by the indentation induced stress. This might cause fracture in the hard coating or brittle film and cause lowering of the hardness. Thus fracture toughness and brittleness plays important role

in case of hard coatings. The critical indentation depth was estimated by power law relation given in Eq. 2.6 [21] where Hf and Hs are the hardness of film and substrate, m=-0.75 and C is normalized critical indentation depth. Thus in the present work, indentation depth was observed to depend on both structure of the coatings and the type of coatings.

$$\frac{h_c}{t} = c(\frac{H_f}{H_m})^{-m} \tag{2.6}$$

In a different approach, scratch resistance of the coatings was conducted by a modified scanning probe microscope [22]. The study was conducted to investigate the effect of substrate, coating thickness and interfacial adhesion on the tribological properties of coating/substrate systems. Micro indentation hardness (MIH) and micro mar resistance (MMR) of the coatings were studied in this system. The two types of specimens were used, hard coatings on soft substrate (Pseries) and soft coatings on hard substrate (Gseries). PECVD coatings were deposited on siloxane/acrylic/polycarbonate multilayer substrates (Pseries) or glass substrates (Gseries) with three different thicknesses.

In MIH test, hardness was observed to depend on the substrate and the critical indentation depth as claimed in previous work. In MMR test, mar resistance of P-series was observed to be better than the G-series. In P-series, the compliant substrate participates in supporting the applied load and thus better is the mar resistance. Damage in hard coatings is seen as micro flaws and cracks whereas in soft coatings the damage is in the form of delamination between coating and the substrate. In P series, as the thickness increased the distribution of stress into the softer substrate got difficult and resulted in cracking in hard coatings. Therefore P series has better MMR for thinner coatings. In G series thicker coatings showed better MMR. From these

experiments, it was observed that by increasing the thickness of the coatings, cracking and delamination can be eliminated and by using the substrate which matches the properties of the coatings, mar resistance can be improved.

b. Numerical Simulations to Measure Hardness

Further research in this field was extended by performing numerical simulations. A study was conducted to simulate nano indentation of soft coatings on hard substrates using Finite element method [23]. A conical indenter was chosen in order to make the same projected area as that of standard Berkovich indenter. Critical ratio of coating thickness to indentation depth (CRTD) in terms of yield strength ratio and indenter tip radius was investigated using FEM.

Simulations were carried out for different tip radius of indenter ranging from r= 0, 0.2, 0.5, 1 and 2 mm. The system was considered to be elastic perfectly plastic. The thickness of the coating was considered to be 1micrometer. As the indenter tip radius increases, the indentation load also increases rapidly. Therefore the indentation process has large influence by the indenter tip radius. On increasing the tip radius, critical indentation depth decreases (CRTD increases). Yield strength ratio of coating to substrate was also seen to have large effect on CRTD, on increasing Yc/Ys (making the coat harder), the critical indentation depth was observed to decrease.

Based on FEA results, an equation was modeled which would give the critical indentation depth where the substrate effect is just 5 percent. The above papers on coatings suggested that the 1/10th rule of critical indentation depth is an approximate and overestimated rule. Critical indentation depth was seen to be dependent on structure of the coatings, brittleness of hard coatings, the tip radius of indenter and the yield strength ratio of coatings and substrate.

2. Scratch Resistance of Polymers

Mar or scratch are the common type of surface damage seen in the polymer. A detailed study of the factors causing these defects and the way to avoid optimize these factors will help in reducing these defects. Studies on polymer materials have suggested that behavior of polymer in nano scale is different from that at micro and macro scale. Work has been done to evaluate the behavior of polymer against surface damage at both nano and macro levels.

a. Scratch Resistance at Nano Level

To shed light on the behavior of polymer materials at nano-scale level, work was done to examine the influence of surface roughness and the indenter tip radius on scratch resistance of polymer [24]. Nano scratch tests were conducted by MTS Dynamic nano mechanical probe system. Experiments were conducted on thermoplastics and thermoset materials.

Under constant load and scratch rate testing condition, it was observed that surface roughness had no or very little effect on the surface damage of the polymer whereas the surface damage was found to be material specific. It was suggested that surface damage of the polymers used as coatings for aesthetic sense to be smaller than the surface it encounters. Mechanical properties of material such as modulus and ductility were found to be important parameters. In nano scratch testing, the higher modulus (achieved by increasing crosslink density) was advantageous while for micro scratch testing, this might lead to higher stresses. Thus these findings were specific to nano mechanical testing of the polymer surface.

The results showed the influence of indenter tip radius on the surface damage of the polymer. The scratch penetration and stress increased on increasing the indenter

tip radius. The surface damage was shown to be controlled, by controlling the testing conditions like indenter tip radius and the load to control the indenter penetration depth. Present work concentrated on testing of polymers at nano level and under constant loading conditions.

b. Scratch Resistance at Macro Level

Various test methods were used in past to characterize the scratch behavior at macro-scale level. The simplest of the test is the pencil hardness test which is most commonly used in industries to characterize the hardness of the coatings. Other sophisticated tests include ford five finger test, pin-on-disc test, taber test, needle test and scratch apparatus. In one of the past research, a new reliable scratch test was introduced which produces consistent and reproducible data with various functionalities [25]. This method had characterized the scratched polymer properties at macro scale level which was one of the major drawbacks in other devices (studied only microscopic or nanoscopic level surface damage). The various factors that affect the scratch behavior of polymers are scratch speed, load on the surface and the fillers present in the material. The new scratch test had the capability to consider all these factors and study their effect independently. New system also executed multi-pass, multi-indenter, constant speed, constant load, increasing speed and increasing load under various ambient temperature conditions.

The equipment consisted of a servo gear driven motor to move the scratch tip under various speed and loading conditions. The stainless steel ball with a diameter of 1mm was used as a scratch stylus tip for scratch length of 100mm. The device was equipped with sensors to sense tangential force, depth, horizontal position and velocity. These data was sent to a computer through data acquisition system for storage and processing. The test parameters during experiment were controlled using

a microprocessor. This device had advantages of providing both dead weight and controlled spring loads (spring loads also prevents chattering of the indenter.), higher speeds for indenter and multiple-indentation when compared to other scratch test devices.

Four different Polypropylene material systems were used. They are homopolymers and copolymers with no talc and talc (20% by wt) fillers. Test were conducted with various combinations of constant load, constant speed, linearly increasing speed and linearly increasing load. After experimentation, TOM (Transmission optical microscopy), SEM and scanned images were used to study the scratch surface damage in terms of scratch width and scratch depths. Finite element analysis was carried out using ABAQUS/Explicit. A 3D model was created and by taking the advantage of plane of symmetry, the specimen was reduced to half of its size along the width. A 3D dynamic and plastic stress analysis was conducted.

During analysis scratch width was taken as the criteria to define the scratch resistance of the polymer under various conditions. Scratch resistance was observed to be more in homopolymer when compared to copolymer which is attributed to the reduced youngs modulus and yield strength of copolymer. The addition of talc filler does not have much effect on the size of the scratch but it alters the mode of scratch damage. Scratch width increased with increasing both load and the speed. Mar-scratch transition was studied and critical load for this transition was determined above which the scratch is visible on the surface of the polymer.

The experimental observations were followed by image analysis and numerical simulations. A commercial image analysis tool VIEEW was used to analyse the scratch. Scratch width at various locations along the scratch length was measured using VIEEW. With the projected area (calculated form scratch width) and load, scratch hardness was calculated for different material systems. At the onset of the

damage, different light reflections called as stress whitening was observed. These were used to characterize the damage and find critical normal load for the onset of scratch.

Finite element analysis package, ABAQUS was used for FE analysis. Symmetry of the problem was utilized and the model was meshed using eight-node linear brick elements. A 3D elasto-plastic stress analysis was executed. The mechanical response of the polymer under scratching was observed. Critical strain criteria were used to predict the regions of the craze/crack propagation [25, 26].

Using this scratch set-up, the effect of coating ductility and coating thickness on scratch resistance was found [27, 28]. The coating with highest ductility was found to show better adhesion than the coatings with lower ductility. With increase in coating thickness, the damage of the coating increased and after reaching a certain coating thickness it levels off. Thus results suggest a critical coating thickness to minimize the damage.

Carlsson conducted research on the thin organic coatings which are used to improve the performance of hot-dip coated steel sheets. They increase the formability of the sheets without additional lubricant and provide corrosion protection. In this paper tribological behavior (friction and wear) of these coatings under forming have been studied. The results from three different tests, pin-on-disc test, modified scratch test and bending under tension test were compared [9].

The two substrate material used were, hot dip coated mild steel with a Zn and 55 % Al-Zn coating. The three thin organic permanent coatings of thickness 1 μm were used. First one was 50 % organic and 50 % non-organic, second was highly organic and low inorganic and third coating was pure organic. Modified scratch test as showin in Fig. 6, was conducted with single as well as triple scratch passes were made and same experiment was conducted three times. Similarly, pin on disc method as shown in Fig. 7, was conducted with a well-controlled multiple circular sliding

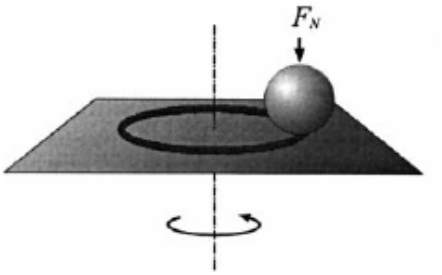

Fig. 6. Pin on Disc Test [9]

motion. In both of these tests, normal and tangential forces were measured using strain gauges. In bending under tension test as shown in Fig. 8, sheet was stretched 90 degrees over a cylinder of radius 5mm. Back tension F2 was applied and F1 was measured. Friction coefficient was calculated and surface topography was studied using Scanning electron microscopy (SEM) and Auger electron microscopy (AEM).

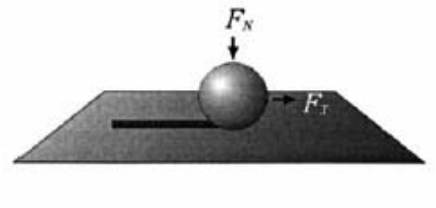

Fig. 7. Scratch Resistance Test [9]

In modified scratch test, coated samples showed lower Coefficient of friction than uncoated samples. Sample with pure organic coatings showed lowest COF. The COF decreased with increase in number of sliding passes for high and pure organic coatings and for others it increased. Similarly in Pin on disc method, all coated samples showed lower initial and steady state COF. The sudden increase in COF after certain number of revolutions was due to the breaking of the thin coatings [29]. In Bending under tension test, there was a fracture in Zn and Al-Zn samples due to very high COF.

Similar to other test, it showed decrease in COF for coated samples. COF was lowest for pure organic coating [30].

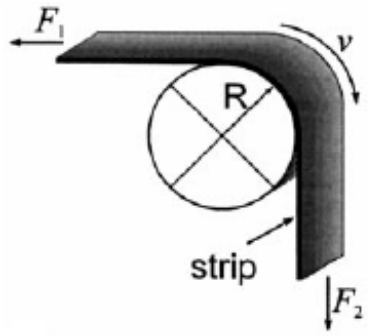

Fig. 8. Bending under Tension Test [9]

Coated samples show good wear resistance than uncoated samples. Pure organic coatings do not undergo much damage when compared to low organic coatings. The welding and material transfer between metal and steel ball occurs after breakthrough of the thin coatings from the substrate. Zn showed adhesive wear mechanism whereas Al-Zn showed adhesive and abrasive wear mechanism. All the three tests showed same results. Small differences in bending under tension was attributed to different geometrical configurations, sliding speed and counter surfaces.

It was concluded that thin film should be deposited with uniform coating thickness, should have high adhesion with substrate, low COF, high load carrying capacity and high wear resistance. Although bending under tension test resembles more closely to the sheet metal forming process, the scratch test and pin on disc test were suggested to be used as they are simpler to perform. These findings led to further investigation of coating thickness and coating composition using scratch resistance test and pin on disc test.

The results from the above tests suggested that both coating thickness and coat-

ing composition can influence the tribological performance of the coatings [31]. Uniform coating coverage should be applied on the surface of the substrate. Coverage of coating was found to be dependent on surface topography of the substrate. Smoother surface topography gave uniform coverage and thus less damage. Relatively thick coatings and smooth surface topography of the substrate were suggested to reduce the breakthrough of the coating.

C. Scope of Present Work

Thus, in past lot of research has been done to evaluate the performance of the coatings under various loading conditions using various parameters. While comparing the results from pin on disc, scratch resistance and bending under tension tests by Carlsson, he only considered material as the parameter. On considering more variables like process parameters, average contact pressure (pin radius), back pressure, lubrication system, sliding velocity and the strain rate, there can be a large variation in the results from these tests. In all the previous studies which uses pin on disc and scratch resistance tests, the performance of polymer coatings was evaluated only based on plastic deformation of the coating. The plastic deformation of the substrate was never considered in these tests. But in bending under tension test, plastic deformation of the substrate is also considered.

Apart from this, bending under tension test has more advantages compared to other two tests. It very closely simulates real forming conditions and as seen from literature, bending plays major role on friction and surface damage. Therefore in the present study, surface and properties of the polymer coatings will be characterized using bending under tension test. Influence of forming variables such as die radius (i.e. contact pressure), lubrication and specimen material will be studied. The present

work is divided into three major parts: 1. building an experimental set-up to simulate real forming process, 2. conducting experiments and data analysis, 3. conducting numerical simulations to analyze specimens in various testing conditions.

CHAPTER III

EXPERIMENTAL SET-UP AND TESTING

Experimental set-up is made to simulate forming of a sheet metal at the die region. The test specimen is stretched and bent around the die corner at an angle of 90°. The bending under tension test is made as shown in Fig. 9. It can adjust the process variables independently like back pressure, average contact pressure and sliding velocity. In the present study, the influence of average contact pressure is studied and that is made possible by changing the die in the set-up. The effect of lubricant is also studied by using different lubricants in the system while keeping other parameters constant. Thus, the set up allows proper control of the parameters desired.

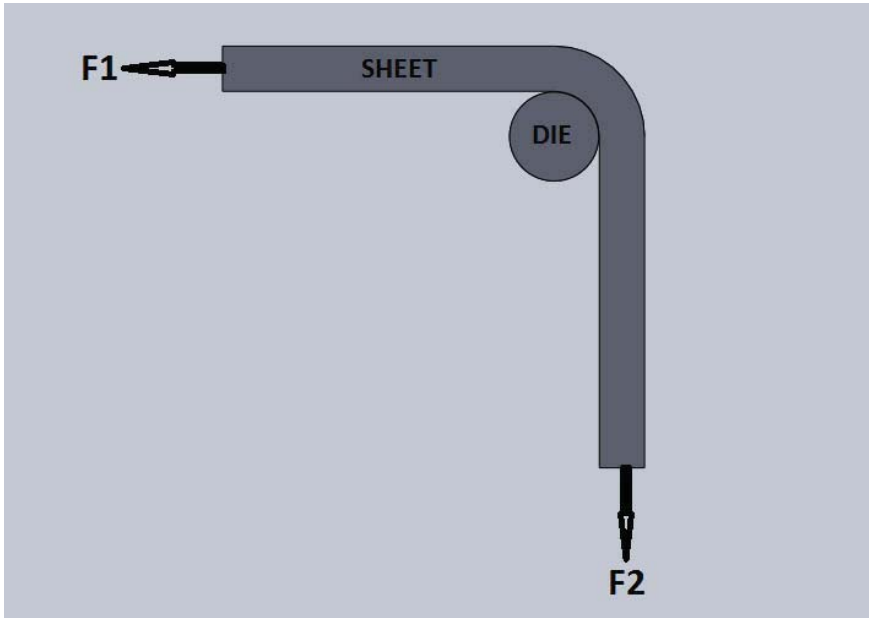

Fig. 9. Bending under Tension Test with 90 Degree Bend Angle

A. Components of the Set-up

The set-up consists of linear actuator, load cells, specimen grips and die assembly. Die assembly consists of die and the die holder. Die is safely secured on the die holder over which the specimen stretches and slides. Hydraulic actuator is used to pull the specimen from one end while back tension is applied with the help of two back plates clamping on the specimen at the other end.

Two load cells are used, one at the pulling side and the other at the back side to measure load values. One end of the Front load cell is attached to the actuator and the other end is fixed to the specimen through the fixture. This load cell can measure the force required by the actuator to pull the specimen. The second load cell is placed at the other end, measuring the clamping load by the back plates. The value of these load cells through data acquisition system is been read into a computer. The set-up is shown in Fig. 10 with individual components discussed in detail.

1. Linear Actuator

Linear displacement actuator is used to stretch and slide the specimen around the die radius. In the present experiment, actuator is driven by hydraulic power system with a capability of maintaining the speed at a desired value. The speed of the actuator is kept constant during the experiment and its value is 8mm/sec.

2. Load Cells

Two load cells are used one at the pulling side and the other at the back side.

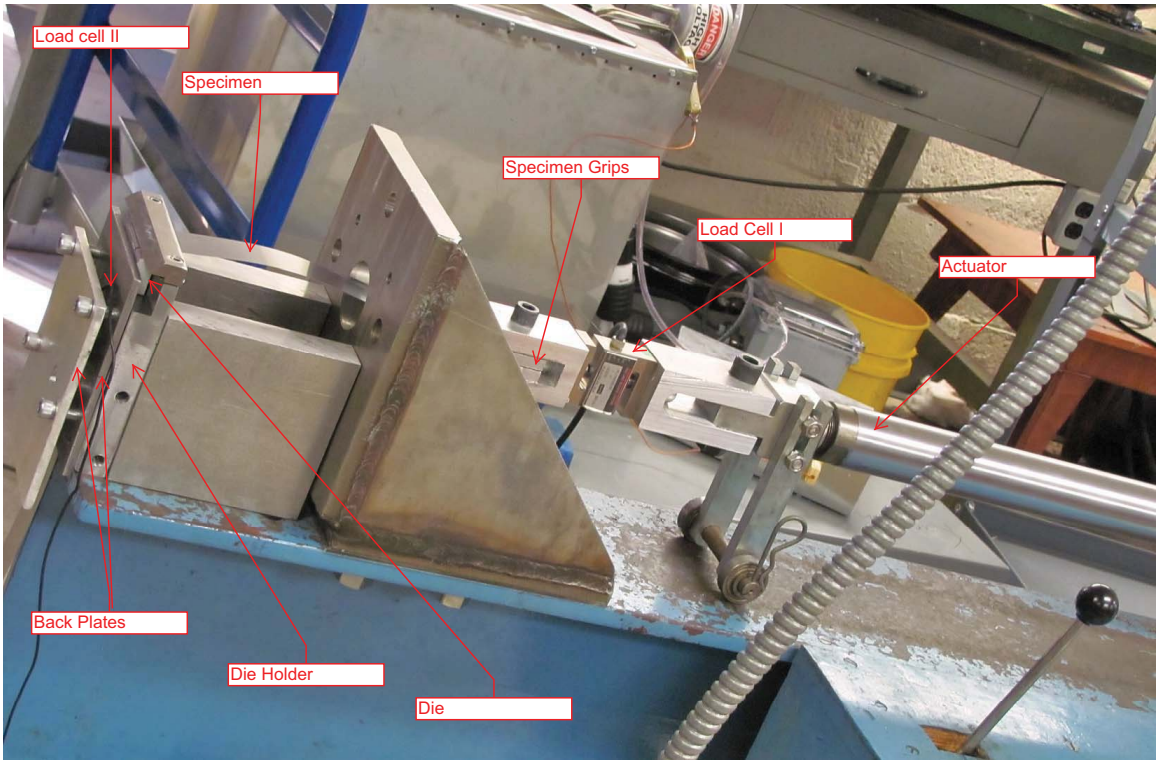

Fig. 10. Experimental Set-up

a. Load Cell to Measure Pulling Force (Load Cell I)

Load cell at the front end is used to measure the force required by the actuator to pull the specimen and was purchased from Loadstar Sensors. It is an S-beam type load cell which can read both tension-compression types of load values. The maximum load that can be read by load cell is 8896.443N (2000lb). It is based on resistive technology and outputs a full scale of 3mV/V. It needs a rated excitation of 10V DC. One side of the load cell is attached to the actuator and the other end is attached to the specimen.

b. Load Cell to Measure Back Clamping Force (Load Cell II)

The load cell at rear end measures the back force applied on the specimen. This load cell was supplied by Loadstar Sensors. The iLoad Mini load cell is based on capacitive technology and outputs a square wave whose frequency is proportional to the applied load. It is a small load cell with height of 6.35mm and diameter of 31.75mm. The size of the load cell makes it best suitable for the present application. The load cell accepts 5V DC input and provides 5V TTL (transistor-transistor logic) frequency output. It is compatible to give both analog and digital output signals. iLoad Mini is a compression type load cell with a capacity of 200lb and an accuracy of 1% of full scale.

3. Data Acquisition System

Data acquisition system was provided by Loadstar Sensors which had capability to acquire the data from load cells and store it in the computer. DQ1000 and DI1000 are two different interfaces used based on the technology used in the load cells. DI1000U is a resistive interface used for S-beam load cell which can convert the existing millivolt

output load cells into PC friendly USB. DI-1000U has an accuracy of 0.02 percent with ADC resolution of 24 bit and 1 channel interface.

DQ-1000 provides a capacitive interface between iLoad Mini series load cell to the PC. The DQ1000 single channel frequency interface provides a simple way to convert the frequency output from the load cell to analog output (DQ-1000A) or a digital output (DQ-1000U). In the present test, DQ-1000U interface is used through which the readings are directly read into the computer via USB. DQ-1000U provides an accuracy of 0.02 percent with ADC resolution of 24bit and 1 channel interface.

LoadVUE (LV) software is used for data acquisition, display and store the load/force values from the load cells. LoadVUE software is compatible with Windows XP/Vista/7 with various applications. In the present application, LoadVUE-4000 is used which can sense upto 4 sensors simultaneously. LV has capability to read load values in lb, kg and g. The other capabilities of LV include total load display, change decimal display, peak and low display. It has the advantage of both logging and plotting the data simultaneously. It can log/plot at the frequency required by the user. It has a speed of 150HZ.

4. Specimen and Gripping Mechanism

Experiments are conducted on the polymer coated metal sheets provided by ATAS International, Inc. Four different types of material samples are provided by the industry. They are: 1. Steel sample of thickness 0.762mm, 2. Aluminum sample of thickness 0.762mm, 3. Textured steel sheet of thickness 0.381mm, 4. Non-textured steel sheet of thickness 0.381mm. The topcoat used on all the samples is polyvinylidene flouride (PVDF) resin commercially named as 70% Kynar 500 / Hylar 5000. Apart from these materials, steel samples with polyethylene coating on either side was also used for testing. The Table. I shows the detail of each sample.

Table I. Specimens for testing

Material	Specimen	Substrate	Material Specification	Grade	Primer and Backer	paint on top side	Sheet Thickness (μm)
Material1	Rawhide	Aluminum	ASTM B209	3003 H14	Polyester	PVDF resin	760.730
Material2	Mission red (non-textured)	Galvanized G90	ASTM A653	SS 37	Polyester	PVDF resin	17.200
Material3	Mission red textured)	Galvanized G90	ASTM A653	SS 37	Polyester	PVDF resin	17.200
Material4	Polypropylene coated metal sheet	Steel	-	-	-	Polypropylene	-

Clamp I and Clamp II are made from aluminum blocks to connect actuator, load cell and the specimen. Clamp I and Clamp II are C-clamps shown in Fig. 10. Clamp I connects actuator to Load cell I and Clamp II connects Load cell I to the specimen. For gripping of the specimen, a hole is punched in the sample which is secured in the Clamp II. Metallic spacers are used in the Clamp II to hold the sheet specimen tightly. The spacers are placed on either side of the sheet specimen to hold it such that the compressive force is enough on the sheet to avoid slipping or tearing of the sheet through the hole while pulling at higher forces.

5. Die Assembly

Die assembly is made to simulate bending under tension test. It consists of a die holder to hold the die, die of different radius, vertical plates to secure die holder to the table and two back plates to apply back force on the specimen passing over the die radius. The assembly is shown in the Fig. 11 and the engineering drawings of the

individual parts are attached in the appendix. The Table. II shows a list of all the parts in the assembly and their uses.

Table II. Components in a die assembly and their functions

No.	Component	Function
1	Die holder	Die holder secures the die and and allows sheet metal to be drawn around the die corner with 90°
2	Die	Die of different radius at its corner is made to draw the sheet over that radius
3	Back plate I	Back plate I is used to apply back pressure on the sheet drawn
4	Back plate II	Back plate II is used to hold the Load cell II
5	Vertical supports	Two vertical plates are used to fix the die holder to the table
6	Top support plate	Supports the sheet at exit from the top when sheet slides over sharp corner

D2 tool steel which has high wear resistance and good corrosion resistance is selected as the die material which can withstand very high contact stresses produced during the test. The die is air hardened and its Rockwell hardness ranges from C17-C21. The die was machined on EDM to give the required profile to it. The die holder is used to secure the die to allow the sheet to pass over the die corner at an angle of

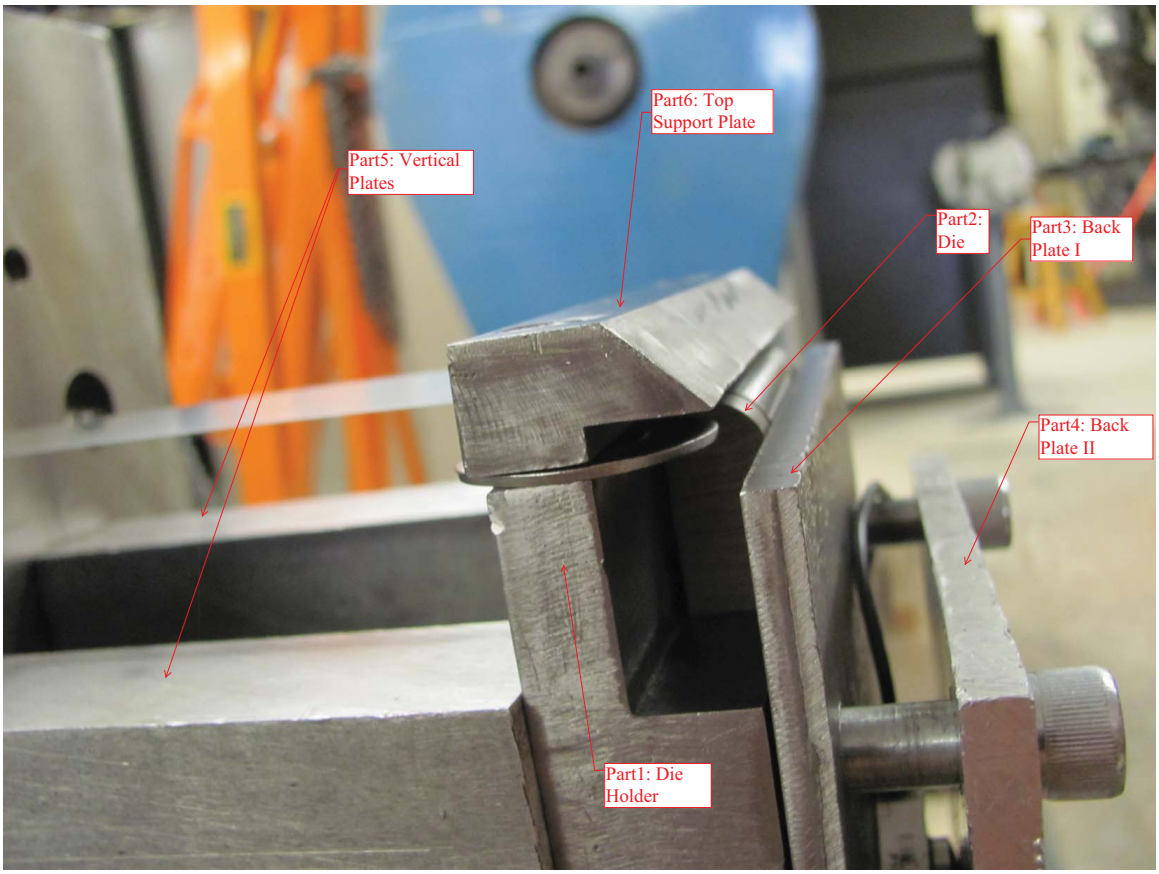

Fig. 11. Die Assembly

90 degrees. The existing die holder was made of 4140 steel and the bulk material was in the heat treated (Annealed) form. The changes were made on this die holder as per the requirements of the current test set-up.

Two Vertical plates were machined from aluminum blocks to hold the die holder to the table. The back tension on the sheet was applied by the back plates. Back plate I was made of 4140 steel which was in contact with the sheet. Back plate II was made of aluminum and was used for securing the Load cell II. Two back plates were secured on the die holder.

B. Test Parameters and Conditions

Bending under tension test is conducted on polymer coated metal sheets. The test is conducted under different parameters while keeping the testing conditions constant for each parameter considered. As mentioned in the literature, there are different test parameters that play a major role during a forming process.

Many parameters and their influence on the final product were investigated in past studies. In the present work, the influence of parameters such as die radius, lubrication and the specimen material is studied on the performance of polymer coated metal sheets when they undergo bending under tension test.

First parameter considered is the die radius. Three different ratio of die radius (r) to material thickness (t) are considered in the present research $r/t=1$(r1), $r/t=5$(r5) and $r/t=10$(r10). The effect of these three different ratios on surface damage, its relation to COF at die interface and the hardness of the coating is studied. Three different die radius are summarized in Table. III.

Lubrication is another important parameter; three different lubricating conditions were tested. Zurn aquasol oil which is commonly used as a machining fluid in

Table III. Die radius

Die Radius	Radius(μm)
r1	760.730
r5	3803.650
r10	7607.300

metal working was purchased from O.F. Zurn Company to use as a lubricant for testing. Three conditions of lubrication were tested, 1. dry condition (without lubricant) 2. 0.01 dilution by weight of zurn oil in water. 3. pure zurn oil without any dilution.

For 0.01 dilution by weight of zurn oil in water the preparation is as follows: Weight of the bucket = 2.25 lb, Weight of Zurn oil + bucket = 2.3125 lb, Weight of Zurnoil+bucket+water = 8.25lb Therefore, Weight of Zurnoil = 0.0625lb Weight of water = 5.9375 lb Dilution by weight = 0.0625/5.9375=0.010526

These three lubricating conditions are considered and tested at *r/t=5*. The other parameter considered was specimen material. The test is conducted to compare the response of different materials. Different materials considered include rawhide material (PVDF coating on aluminum substrate), PP coating on steel sheet, Mission red non textured (PVDF coating on steel substrate), Mission red textured (PVDF coating on steel substrate). All these parameters are summarized in the Table. IV.

All the tests are conducted while maintaining certain test conditions. In all the tests, the sheet is pulled by an actuator with constant speed of .During the test, back pressure is maintained at a constant force value of 750N. Before conducting every test proper care is taken to remove any dirt or particles from the surface of the die and the sheet. After testing, COF is calculated from the forces measured by the load cells, polymer coating is characterized by different material characterization techniques.

Table IV. Test matrix

Study	Parameters									
	Radius of the die to thickness ratio(r/t)			Lubrication Condition			Specimen Material			
	r/t=1 (r1)	r/t=5 (r5)	r/t=10 (r10)	Dry	1% Dilution	No Dilution	Material1	Material2	Material3	Material4
Friction Coefficient	-	✓	✓	✓	✓	✓	-	-	-	-
Optical Microscope	✓	✓	✓	✓	✓	✓	✓	✓	✓	✓
Nanoindentation	✓	✓	✓	-	-	-	✓	-	-	✓
Thickness	✓	✓	✓	-	-	-	-	-	-	-

C. Friction Model and Material Characterization Techniques

1. Friction Model

Wilson and Saha's friction model based on system force balance is used to calculate Coefficient of friction (COF). This model takes into account the angle of contact and the force due to bending. The model for COF is given by the Eq. 3.1 [16].

$$\mu_d = \frac{2}{\theta}\left(\frac{F1 - F2 - F_b}{F1 + F2}\right) \tag{3.1}$$

where μ_d = Coefficient of friction at die and sheet interface, θ = Angle of wrap, F1= Front tension, F2= Back tension, F_b= Bending force given by Eq: 3.2 [13]

$$F_b = \frac{\sigma_y\, t^2\, W}{2r} \tag{3.2}$$

where σ_y = Yield strength of the strip, W=Width of the strip, t=Thickness of the strip and r=Radius of curvature

In the present case, θ = angle of wrap = 90°, F1 is the force measured by Load cell I to pull the strip by the actuator, F_b is the bending force which is calculated from yield st, radius of curvature, width of the specimen and thickness; which is known

and F2 is the back tension calculated from the back force measured by the load cell II. Load cell II in the experiment measures the normal force applied by the back plate on the sheet. To calculate the back tension, normal force is multiplied by friction coefficient between the back plate and the sheet material given by Eq. 3.3:

$$F2 = \mu_b N \tag{3.3}$$

where F2 = back tension, μ_b= COF between back plate and sheet, N = load measured by Load cell II.

μ_b is also calculated using the same set-up for bending under tension test with some variations in the set-up. The sheet is pulled in between two plates similar to bending under tension test but without bending to calculate μ_b. The ratio of pulling force calculated by the actuator to the weight of the back plate kept on top of the sheet gives the μ_b. The values for COF is given in Table. V. Thus, F2 is calculated

Table V. COF between sheet and back plate

Trial No.	COF (μ_b)
1	0.207
2	0.177
3	0.151
Average	0.178

from Load cell II and is kept constant under all parameters and conditions during testing. Finally μ_d is calculated with system force balance model which also considers the contribution due to bending.

2. Optical Microscope

Optical microscope was used which has the capability to take the images at different resolutions of 5X, 10X, 20X, 50X and 100X. Pictures of the specimen before and after the test were taken. Optical microscope helped in providing detailed and clear pictures of the specimen surface for comparison.

3. Nano Indentation

Nano indentation is a powerful tool used to measure the mechanical properties of the material at nano scale. It is a depth sensing technique in the sub micrometer range which can measure hardness, modulus and other mechanical properties.

Nano indentation was made possible by use of a machine that can make tiny indentations while recording load and displacement values and analyzing these data by models to obtain mechanical properties of the material with good precision and accuracy. In the present study, the hardness of the polymer coating was investigated with Nano indentation technique.

Triboindenter was used to perform indentation test and find the hardness of the polymer coatings [32]. It is used for nano mechanical testing which has the capability to perform automatic testing as well as take in-situ images.

Tribo scan 5.0 software is used to control all the functions of triboindenter. All the normal tasks of the triboindenter are automated by use of this software however it is also designed to be flexible enough for complicated tasks.

Working with triboindenter involves three basic steps:

1. System set-up and Calibration

2. Load function and Sample navigation

3. Data analysis

The first step involves setting up the system by turning on stage, scanner, transducer controllers, vibration isolation control unit, mirror control unit and optical light. This is followed by setting up the values manually for transducer controllers as desired and setting similar values in Tribo scan software. Air indent calibration is a very important step to be performed before doing any indentation test. Air indent is performed in order to keep the electrostatic force constant at a particular value in spite of changes in masses of tips or leveling.

The second step involves setting up the load function and sample navigation. Once the sample is mounted on the stage, a load function is defined in the load editor. The load applied by the indenter to the sample is function of time and this graph is described in load function. The load function is composed of linear segments where first segment starts at zero force and last segment ends at zero force. The software has the ability to add up about 50 segments. Besides linear segments, sinusoidal segments are also an option.

In sample navigation, the positions and patterns on the sample are selected. The triboindenter has ability to perform single indentation or multi indentations. A particular method utilizes one loading function. The load in a method is adjusted for every progressive indent in four different ways. They are: 1. Adjust peak load while keeping load rates constant 2. Adjust peak load while keeping segment times constant. 3. Adjust loading rates while keeping peak load constant and 4. Adjust time at peak load keeping all other segments constant. In the present case for a given load function and method, the peak load is adjusted while keeping segment times constant.

The final part involves analysis of the data obtained by nano indentation test.

After testing, the load-depth curve is plotted. Using a portion of the unloading curve, a power law is fit as given in Eq. 3.4.

$$P = A(h - h_f)^m \tag{3.4}$$

where P is load applied, h is indentation depth, h_f is the residual plastic deformation and A is the projected contact area.

The derivative of power law relation with respect to h gives contact stiffness $S = dp/dh$. The contact depth hc is calculated by the equation given in Eq. 3.5

$$h_c = h_{max} - 0.75(\frac{P_{max}}{S}) \tag{3.5}$$

where h_c is the contact depth, h_{max} is the maximum indentation depth, P_{max} is the maximum load applied and S is the stiffness.

The Hardness from contact depth (h_c) is calculated as given by Eq. 3.6.

$$H = \frac{P_{max}}{Ah_c} \tag{3.6}$$

The reduced modulus is calculated as given by Eq. 3.7.

$$E_r = \frac{\sqrt{\pi}}{2\sqrt{Ah_c}}(S) \tag{3.7}$$

Triboscan software also has the capability to perform multianalysis of load vs depth curves. After analyzing all the curves, hardness and reduced modulus are plotted as function of contact depth.

4. Surface Roughness Measurements

Surface roughness of the die is measured before conducting the experiments to make sure that all the dies of different radius have similar surface roughness values. Contact

type surface profilometer is used to measure the surface roughness value. In contact profilometers, a stylus is moved normal to make contact with the surface of the specimen and then moved parallel to the surface.

The variations on the surface of the specimen are detected as function of vertical stylus displacement at various positions. These analog signals are then converted into digital signals, analyzed and displayed. The mean surface roughness value of the specimen is recorded in the present case is given by Table. VI.

Table VI. Surface roughness of the die

Die Radius	Surface Roughness(μm)
r1	0.934
r5	1.184
r10	1.000

CHAPTER IV

EXPERIMENTAL RESULTS AND DISCUSSIONS

A. Friction and Surface Damage

Coefficient of friction at die and sheet interface is calculated by Wilson and Saha's model. Surface irregularities on the coating surface after the test are studied using optical microscope and images from camera. The effect of individual parameters on friction and surface damage is discussed in subsequent sections.

1. Effect of Die Radius

a. Force Comparison

The effect of die radius to thickness ratio was studied on Material1 under dry lubricating condition. Ratio of die radius to sheet thickness *r/t=1* corresponds for radius *r1*, *r/t=5* for *r5* and *r/t=10* for *r10*. The effect of *r1*, *r5* and *r10* on the force required to pull the strip is shown in Fig. 12.

The graph shows the variation in front tension (F1) for different die radius while maintaining the back tension (F2) at a constant value of 133N. As the die radius decreases, the force required to draw the specimen around the die corner increases. This can be attributed to two factors, increase in force due to bending and increase in frictional force at the die region. The force required to pull the specimen has to overcome three basic forces, the force balance is shown in Eq. 4.1:

$$F1 = F_b + F_f + F2 \tag{4.1}$$

where F1 is the force required to pull the specimen, F_f is the frictional force at the die radius, F2 is the back tension (which is kept constant) and F_b is the force required

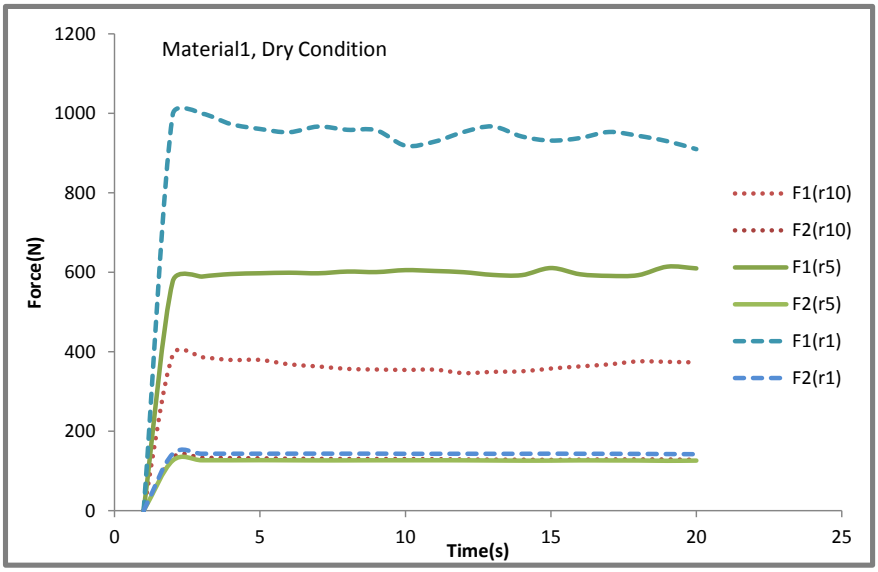

Fig. 12. Force Curves

to bend the specimen around die corner.

Bending force is inversely proportional to the die radius. Thus, as the die radius decreases, bending force increases and which in turn increases the pulling force. The effect of frictional force can be clearly understood by studying the COF at the die region which is discussed in next section.

b. COF Comparison

Fig. 13 Shows the variation of COF with die radius for Material1 under dry lubrication condition. The graph shows the COF for *r10 (r/t=10)* and *r5 (r/t=5)* for two trials. It is clearly seen that for *r10*, the COF is less when compared to *r5* die radius. Thus with decrease in die radius, COF increases.

The increase in COF for *r5* die radius is due to increase in contact pressure. As die radius decreases, the contact pressure at the die and the sheet interface increases due to an increase in true contact area between the sheet and the die. Thus, with

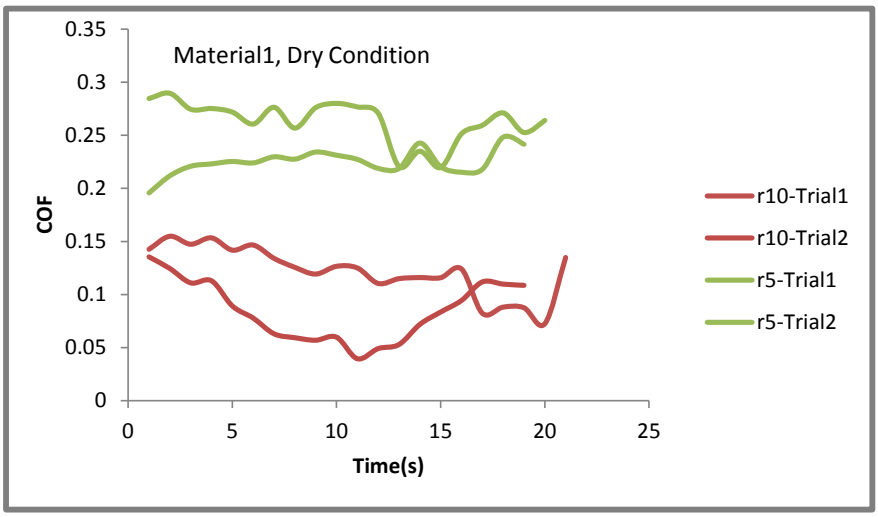

Fig. 13. COF Curves

decrease in die radius, COF increases which causes increase in pulling force observed in previous section. Therefore, change in die radius influences both frictional force and bending force.

It is also interesting to note that the friction coefficient is not constant during the test. It varies within the test, explaining dynamic nature of the friction coefficient. There is slight variation seen in friction coefficient between two trials and is observed because of variations seen in back tension during the test. The mean COF calculated for *r5* and *r10* die radius is shown in Table. VII.

Table VII. COF for r5 and r10 radius

COF	r5	r10
Trial1	0.263	0.122
Trial2	0.225	0.085
Mean COF	0.244	0.104

c. Surface Images

Surface images of the Material1 were taken before and after the test by optical microscope and camera. Images taken form camera are shown in Fig. 14.

Fig. 14 shows the surface condition of Material1 before and after the test for different die radius. Fig. 14(a) shows the surface condition of the specimen before testing. Fig. 14(b) shows the surface condition of the specimen after drawing it over r10 die radius. In this case, distinct stretching in drawing direction is observed. Similarly, for r5 die radius stretching with few light scratches on the surface are observed as shown in Fig. 14(c). For r1 radius shown in Fig. 14(d), scratches on the surface in drawing direction after the test are clearly seen.

The images taken form optical microscope gives more detailed information of surface condition as shown in the Fig. 15. The changes in the form of stretching and scratches on the surface were observed.

A relation is seen between the surface damage of the polymer coatings observed and the friction coefficient calculated. More damage observed on the surface of the coatings with r5 die radius also showed higher COF when compared to r10 die radius. Thus, lower COF resulted in lesser change on the surface as expected. And sharper the die radius, higher is the COF and surface damage in the polymer coating.

2. Effect of Lubrication

Three different lubricating conditions dry, dilution of zurn oil in water (1%) and pure zurn oil without any dilution were tested using Material1 and die radius r5.

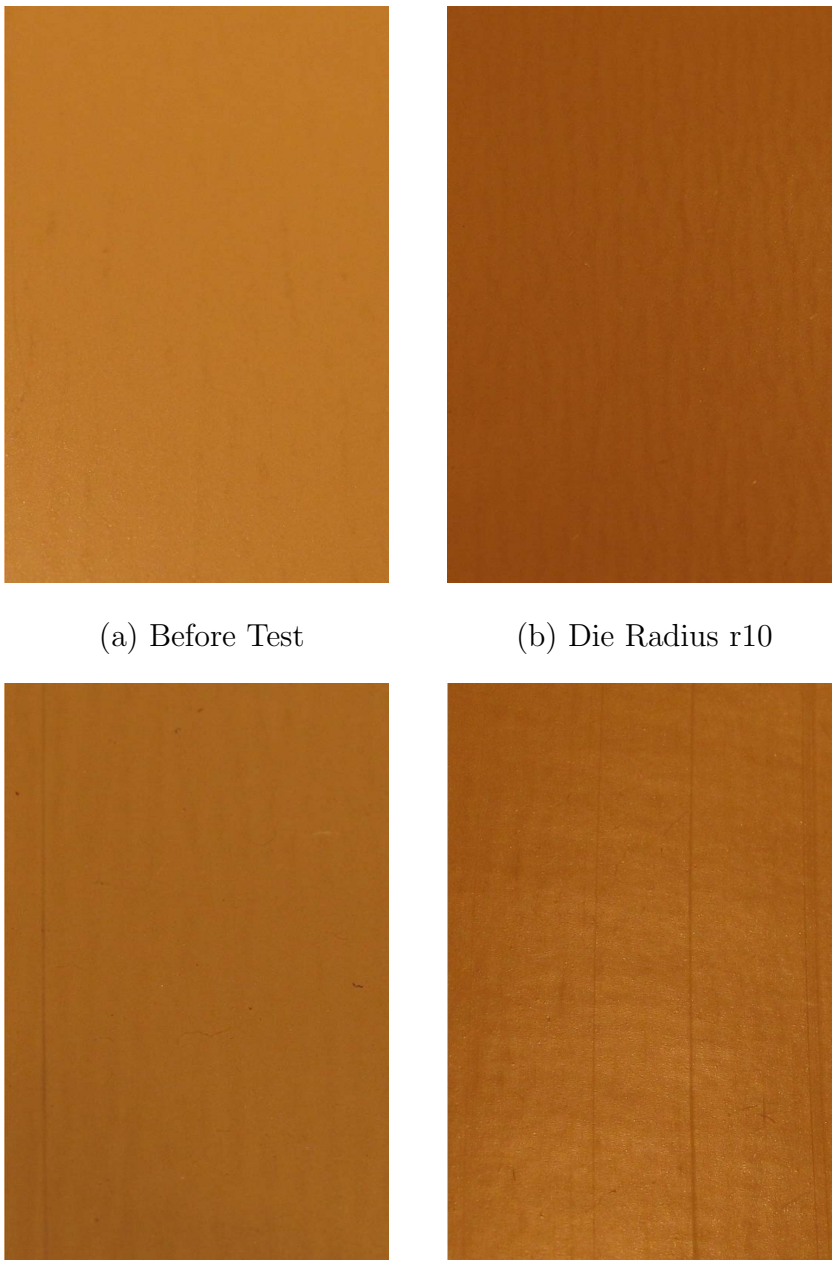

(a) Before Test (b) Die Radius r10

(c) Die Radius r5 (d) Die Radius r1

Fig. 14. Surface Condition of Material1 Before and After the Test for Different Die Radius

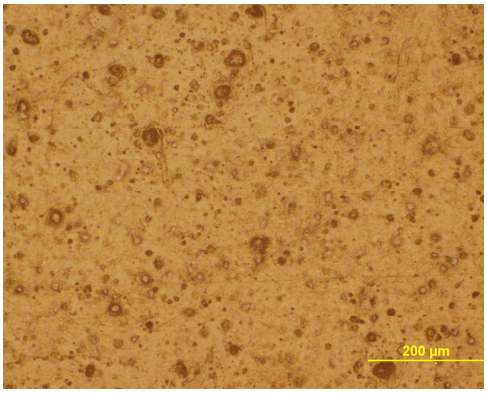

(a) Before test

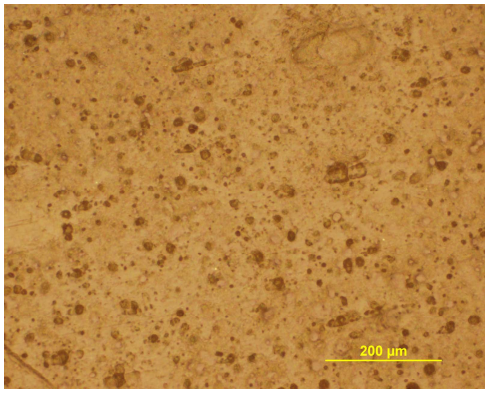

(b) Die Radius r10

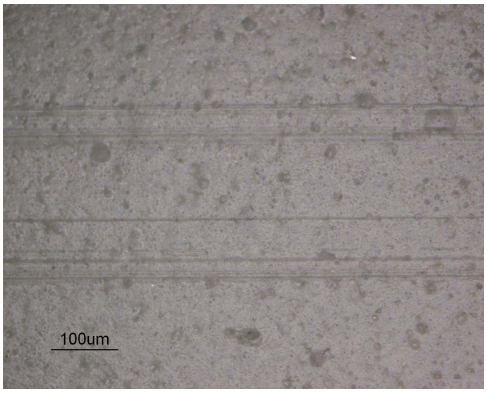

(c) Die Radius r5

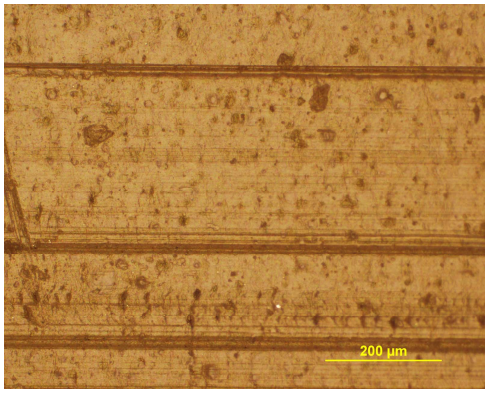

(d) Die Radius r1

Fig. 15. Surface Images Using Optical Microscope for Material1 Before and After Test

a. Force Comparison

Fig. 16 shows front and back tension for three different lubricating conditions. The back force is maintained at constant value of 133N for all the three tests and front tension is measured.

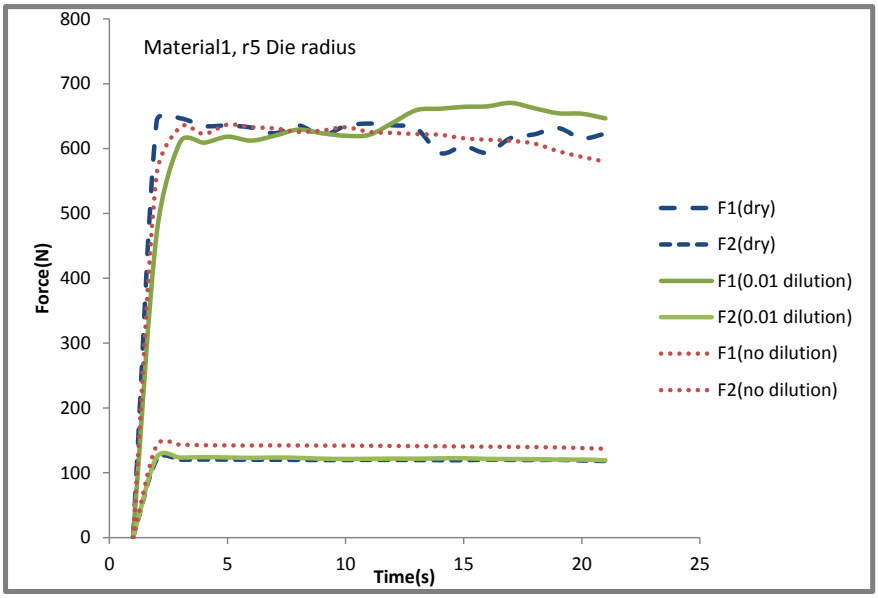

Fig. 16. Force Curves

As shown in Fig. 16 there is not much difference seen in the force required to draw the specimen under different lubricating conditions. The polymer coating itself acts as a solid lubricant in the test and thus there is not much difference seen on using additional lubricant.

b. COF Comparison

Fig. 17 shows the variation in COF under dry and diluted lubrication conditions. COF is less for diluted condition than dry condition. But the effect of lubricant is not much as that of die radius on COF.

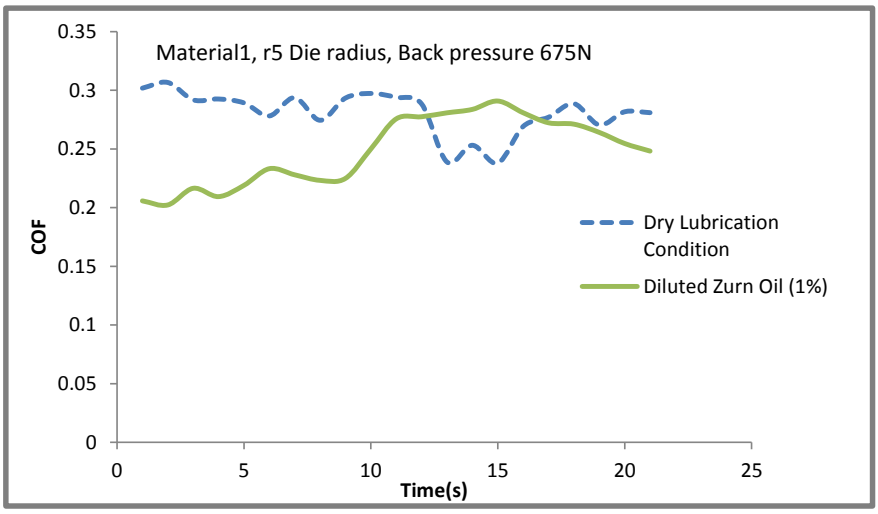

Fig. 17. COF for Dry and Diluted Lubrication

Fig. 18 shows the variation in COF under 1% dilution of lubricant in water and no dilution of lubricant. It is observed that the COF for no dilution is lesser than 1% dilution as expected. It is also interesting to observe in Fig. 17 & Fig. 18 that the friction coefficient for 1% diluted lubricant increases during the test with time. This is due to less viscous nature of the diluted lubricant. With time, the lubricant is squeezed out and thus causes increase in COF.

Fig. 19 shows variation of COF for all the three lubricating conditions. The back tension of dry and diluted conditions are kept at same value whereas for pure lubricant (no dilution), back tension was maintained at slightly higher value. Similar to above observations, COF is highest in case of dry lubricant followed by diluted lubricant and lowest in case of pure lubricating condition. In spite of higher back tension in pure lubricating condition, COF was observed to be lower. Though lubrication has some effect on the COF, the influence is not as significant as that of die radius.

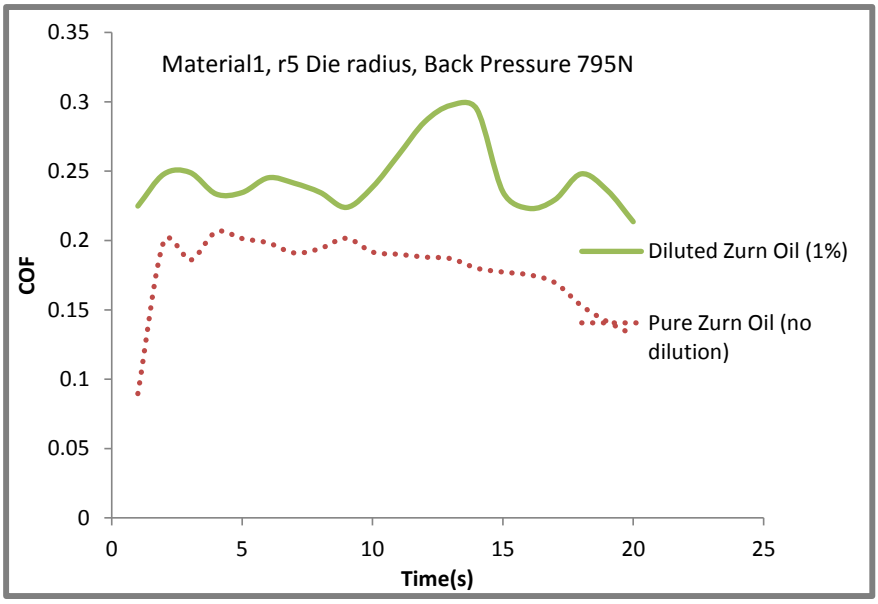

Fig. 18. COF for Diluted and Pure Lubrication

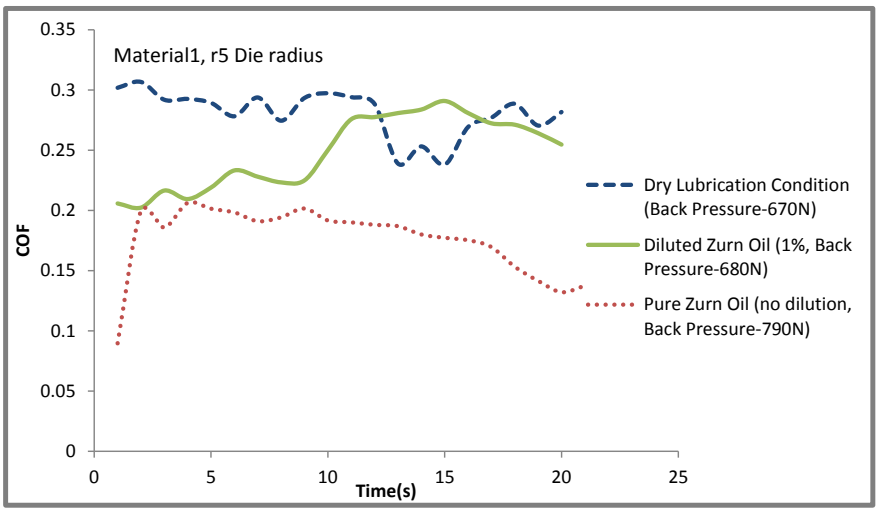

Fig. 19. COF for Dry, Diluted and Pure Lubrication

c. Surface Images

Surface images were taken by microscope and are shown in Fig. 20. As observed from force and COF calculations, the effect of lubrication in not very significant. Figure shows the variation on the surface under dry, diluted lubricant and lubricant without dilution. Surface in case of lubricant without dilution looks more glossy and clear, diluted lubricant surface is also similar but with very light scratches on the surface.

3. Effect of Material

To compare the materials, test were conducted on Material4 (Polypropylene coated metal sheets) and Material1 (PVDF coated metal sheets). Hardness of these two materials were calculated before test using Nano-Indentation test as shown in Table. VIII. Hardness of the coating used for Material4 is lower than the coating used for Material1. Both the sheets were drawn over die radius *r1*, *r5* and *r10* under dry lubrication condition. Fig. 21 shows the surface images of two different materials after testing.

Table VIII. Hardness comparison of Material1 and Material4

Material	Hardness(GPa)
Material1	0.200
Material4	0.092

Material4 shows more damage when drawn over all the die radius compared to Material1. Polypropylene being the softer material when compared to PVDF coating is observed to have more scratches on the surface when drawn over *r1* die radius. For

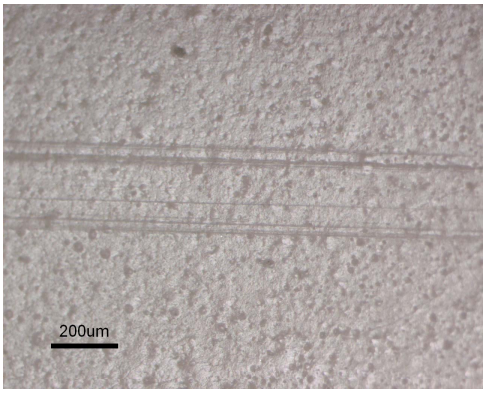

(a) Dry Condition

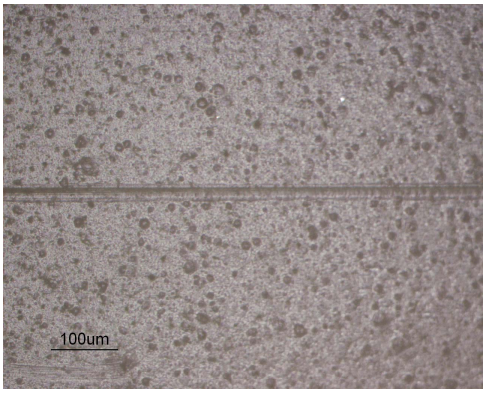

(b) Diluted Lubricant

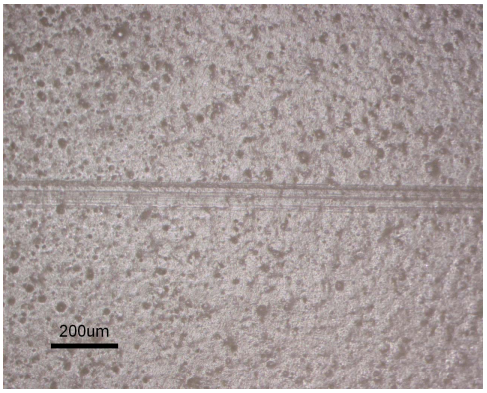

(c) Lubricant without Dilution

Fig. 20. Surface Images Using Optical Microscope for Different Lubricating Conditions

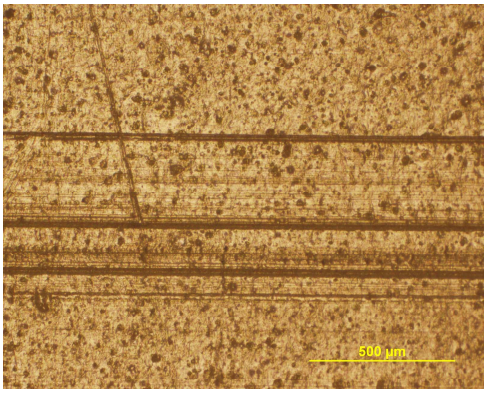

(a) Material1 drawn over r1 radius

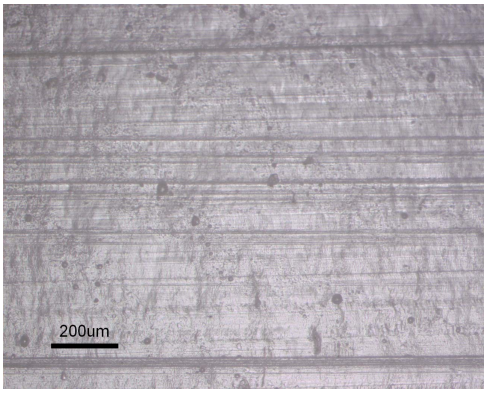

(b) Material4 drawn over r1 radius

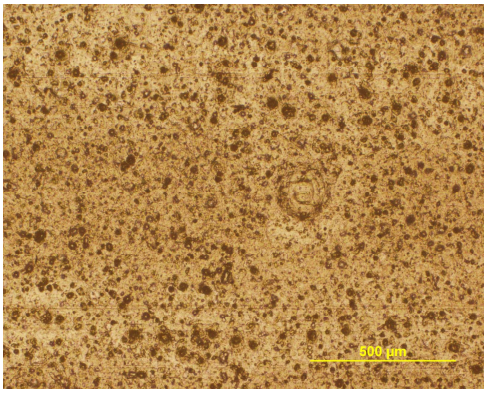

(c) Material1 drawn over r5 radius

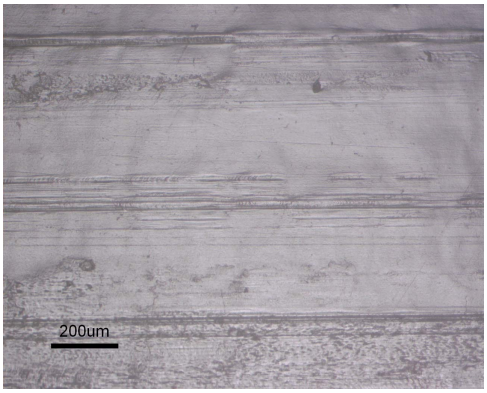

(d) Material4 drawn over r5 radius

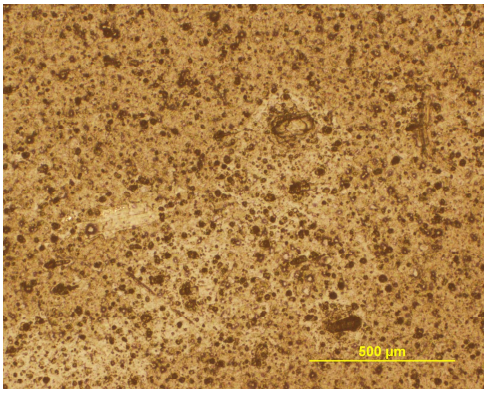

(e) Material1 drawn over r10 radius

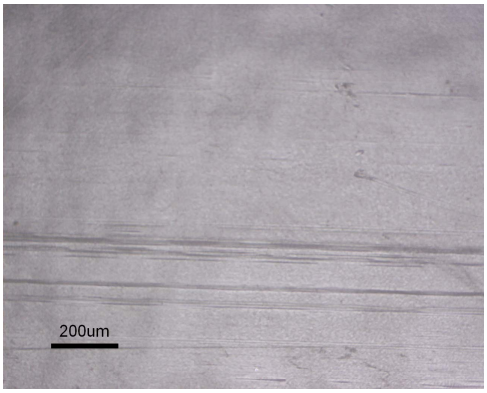

(f) Material4 drawn over r10 radius

Fig. 21. Surface Images Using Optical Microscope for Different Materials

r10 die radius, PVDF coating showed no scratches on the surface but scratches were seen for Polypropylene material. Thus, properties of material does make a difference when drawn under different forming conditions.

Apart from comparing two different materials, same materials but with different surface topography were also compared. Material2 which is a non textured material was compared with Material3 with textured surface. Fig. 22 shows the surface images for Material2 and Material4.

As observed in Fig. 22, both textured and non-textured surfaces shows no damage for r10 die radius. Textured surface shows damage when drawn under r5 die radius which is not seen for non-textured surface. The protrusions formed during texturing are scratched off while drawing under r5 die radius as the contact pressure increases. Similarly, while drawing Material3 (textured) over r1 die radius, contact pressure increases further, leading to more surface damage. Both textured and non-textured surfaces show higher damage in case of r1 radius. Thus, textured and non-textured surfaces shows different behavior under drawing.

B. Hardness of the Coating and Thickness Change of the Sheet

Hardness of the coating was measured for Material1 before and after the test to check for its property change. Thickness measurements were also conducted to find the strain produced in the material after testing.

1. Effect of Die Radius

a. Hardness Study

The effect of die radius on the properties of the polymer coating was characterized by measuring the hardness of the polymer coatings using nano indentation test. Multi

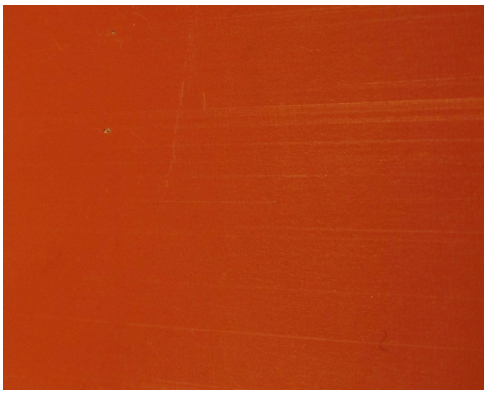

(a) Material2 drawn over r1 radius

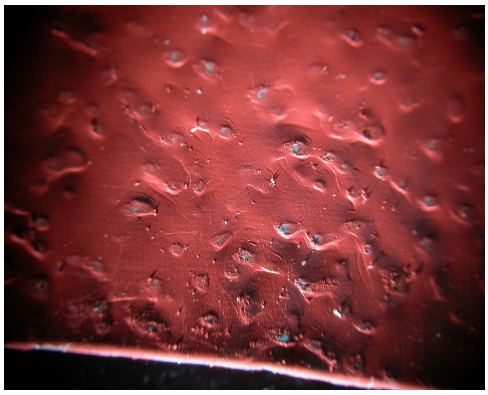

(b) Material3 drawn over r1 radius

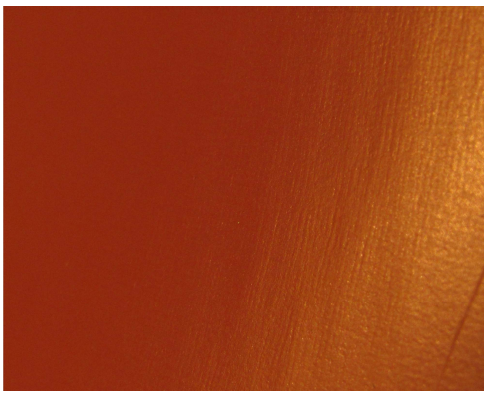

(c) Material2 drawn over r5 radius

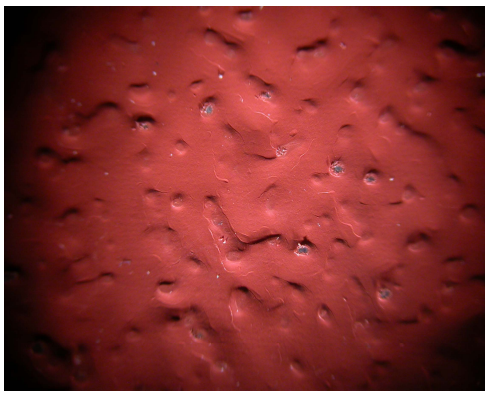

(d) Material3 drawn over r5 radius

(e) Material2 drawn over r10 radius

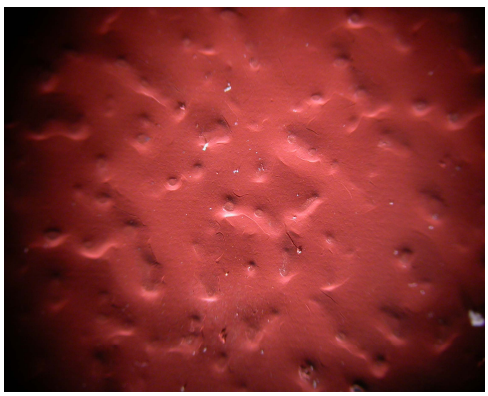

(f) Material3 drawn over r10 radius

Fig. 22. Surface Images Using Optical Microscope for Textured and Non-Textured Materials

indentation test was carried out for finding the hardness at different depths for the coating. Table. IX shows hardness of the polymer coating at different depths before test.

Table IX. Hardness of coating before test

Test No.	Pmax(μN)	hmax(nm)	hc(nm)	A(nm^2)	H(GPa)
1	10207.799	1490.992	1374.521	53623551	0.190
2	10200.895	1468.317	1349.479	51770304	0.197
3	8106.061	1240.652	1138.423	37408286	0.217
4	6048.977	1073.468	985.282	28400462	0.213
5	4004.341	941.614	861.280	21983279	0.182
6	8066.008	970.438	865.375	22182588	0.364

In the Table. IX, Pmax is the maximum load applied by the indenter, hmax is the maximum depth traveled by indenter,hc is the contact depth, A is the area calculated from hc and H is the hardness calculated.

Table. X shows hardness of the polymer coating after drawing under *r10* die radius. Each of these values in table, summarizes hardness values at different depths.

Table. XI shows hardness of the polymer coating after drawing under *r5* die radius and it summarizes hardness values at different depths.

Table. XII shows hardness of the polymer coating after drawing under *r1* die radius. Each of these values in table, summarizes hardness values at different depths.

Table X. Hardness for r10 die radius

Test No.	Pmax(μN)	hmax(nm)	hc(nm)	A(nm^2)	H(GPa)
1	10177.064	1351.329	1244.905	44372885	0.229
2	10198.815	1487.926571	1370.541	53326895	0.191
3	10216.542	1558.621	1460.655	60238807	0.170
4	8063.326	973.794	872.948	22553491	0.358
5	8061.242	1023.902	919.842	24915772	0.324
6	8068.017	1103.007	1006.889	29599063	0.272

Table XI. Hardness for r5 die radius

Test No.	Pmax(μN)	hmax(nm)	hc(nm)	A(nm^2)	H(GPa)
1	930.062	482.549	444.598	6260673	0.148
2	10215.77	1539.571	1412.329	56481285	0.181
3	10207.78	1507.605	1390.786	54844135	0.186
4	935.981	454.855	418.598	5584507	0.168
5	939.523	424.165	385.292	4772150	0.197
6	8088.888	1419.249	1313.377	49154185	0.164
7	4452.311	1074.317	989.168	28614301	0.156
8	8078.9	1170.817	1053.743	32279955	0.250
9	8071.939	1144.175	1038.85	31415693	0.257

Table XII. Hardness for r1 die radius

Test No.	Pmax(μN)	hmax(nm)	hc(nm)	A(nm^2)	H(GPa)
1	10208.97	1596.882	1487.022	62338363	0.164
2	7053.271	1305.081	1213.901	42285831	0.167
3	3947.37	1037.871	965.308	27313664	0.144
4	931.507	482.566	439.681	6130003	0.152
5	7055.32	1504.887	1409.93	56297875	0.125
6	3950.648	994.332	917.211	24780276	0.159
7	960.235	289.15	261.903	2299181	0.418
8	10226.82	1672.401	1561.945	68494914	0.149
9	7054.048	1319.499	1223.795	42946574	0.164
10	3950.021	988.963	910.083	24414895	0.162
11	926.244	517.961	482.508	7312119	0.127
12	4998.826	589.323	543.967	9180343	0.544
13	4986.051	972.387	894.222	23611184	0.211
4	10157.54	1087.387	1012.466	29912332	0.339
15	960.235	289.15	261.903	2299181	0.418
16	4998.826	589.323	543.967	9180343	0.544

Table XIII. Hardness values

Parameters	Hardness(GPa)
Before test	0.200
r10	0.197
r5	0.171
r1	0.151

As observed from hardness measurements in Table. XII, hardness values for test 15 and 16 are high. The positions for test 15 and test 16 are the scratch positions, that increased the hardness value due to the influence of substrate. In addition to this, it is also interesting to know that hardness for all the specimen increases at a particular load value and this can be explained by the presence of fillers in the polymer coatings.

Table. XIII summarizes the hardness measured for the coating before and after the test with different die radius.

The Table. XIII clearly shows that hardness of the polymer coating decreases when drawn with sharper die radius. Softening of the polymer takes place when drawn around sharper die radius.

b. Thickness Study

Change in the thickness of the specimen is measured after the test with micrometer and the values are shown in Table: XIV.

The percent change in thickness of the sheet is highest in case of r1 radius followed by r5 and r10. Assuming, there is no change in volume of the specimen, the sum of the strains in all three directions sum up to zero as shown in Eq. 4.2:

Table XIV. Thickness values

	Before Test	r10	r5	r1
Thickness(mm)	0.761	0.751	0.733	0.709
% change in thickness	0	1.314	3.679	6.833

$$\epsilon_{longitudinal} + \epsilon_{lateral} + \epsilon_{transverse} = 0 \tag{4.2}$$

where $\epsilon_{longitudinal}$ is the strain in drawing direction, $\epsilon_{lateral}$ is the strain in width direction and $\epsilon_{transverse}$ is the strain in thickness direction.

Assuming, $\epsilon_{lateral}$ is negligible and approximating it to zero, results in $\epsilon_{longitudinal} = \epsilon_{transverse}$. Thus, strain in the sheet produced in the drawing direction is same as % change in the thickness. Strain in longitudinal direction for r1 radius is highest as thickness change is maximum for r1 radius. Higher friction and higher bending force required to pull the strip around r1 radius produces higher strain.

Experimental Studies, helped in knowing the parameters, that can affect the performance of polymer coatings. Effect of die radius, lubrication and material were studied in detail in this chapter. Apart from experiments, numerical simulations are necessary to get more insight into the process and find reasons for surface damage. Numerical simulations are discussed in detail in next chapter.

CHAPTER V

NUMERICAL SIMULATIONS

A. Introduction

Numerical simulations are used to evaluate the mathematical model of a process and estimate its characteristics. It is an easy and efficient way to solve and provide approximate solutions to a problem. The present work aims at simulating the experiment using numerical method and comparing the results to get a better understanding of the problem. These simulations were further used to change the variables independently and predict the results just by performing numerical simulations (without running experiments).

The plane strain FEM simulations for bending under tension test were performed using Finite Element Analysis package (FEA) ABAQUS. The model for the simulations is made similar to the experiment set-up and the conditions are maintained as that of the experiments. The influence of die radius on the performance of polymer coated metal sheets was studied. Simulations were conducted for die radius to thickness ratio of $r/t=5$ and $r/t=3$. The results from $r/t=5$ were compared with experiment results to check for its validity. After checking for the validity, simulations were conducted for $r/t=3$ to predict its results.

Strain in the specimen, force required to pull the specimen and contact pressure were measured from the numerical simulations. Strain values measured from FEA results are compared to the strain obtained from experiment results to check for validity of FEA simulations. This can also be used as a criteria to predict the damage of the coating. Contact pressure evaluation helps in studying the pressure distribution when the sheet passes over the die radius. Critical positions of peak pressure is

determined.

B. Geometry and Model

Model is created in ABAQUS for bending under tension test which is shown in Fig. 23 where the sheet is bent and drawn around the die radius. A 2D model is made by exploiting the plane strain behavior of the sheet across the width direction. ABAQUS Explicit is used to conduct analysis. The sheet, die and the two back plates are modeled as separate parts. Die and Back Plates are modeled as discrete rigid surfaces with RIGID BODY option. The sheet is modeled as a deformable body made of two layers. First layer is the substrate material of thickness 0.73787 mm and other layer is of coating material of thickness 0.02286 mm. The sheet material is meshed using biased meshing option. This option will give finer mesh in the coating region and coarser mesh in the substrate region. Linear quadrilateral element is used to mesh the whole model. Die radius of 3.804mm is modeled to simulate the condition of $r/t=5$ and die radius of 2.282mm is modeled to simulate $r/t=3$.

C. Material Model

An elastic-plastic isotropic material model is used to define the material behavior of the sheet. Two solid homogeneous sections were created, one for substrate and other for coating. Substrate material was defined as Aluminum of grade 3003-H14 whose material properties were obtained by tensile testing of the as received material as shown in Table. XV. While material properties for coating material PVDF is obtained from literature [33] as shown in Table. XVI.

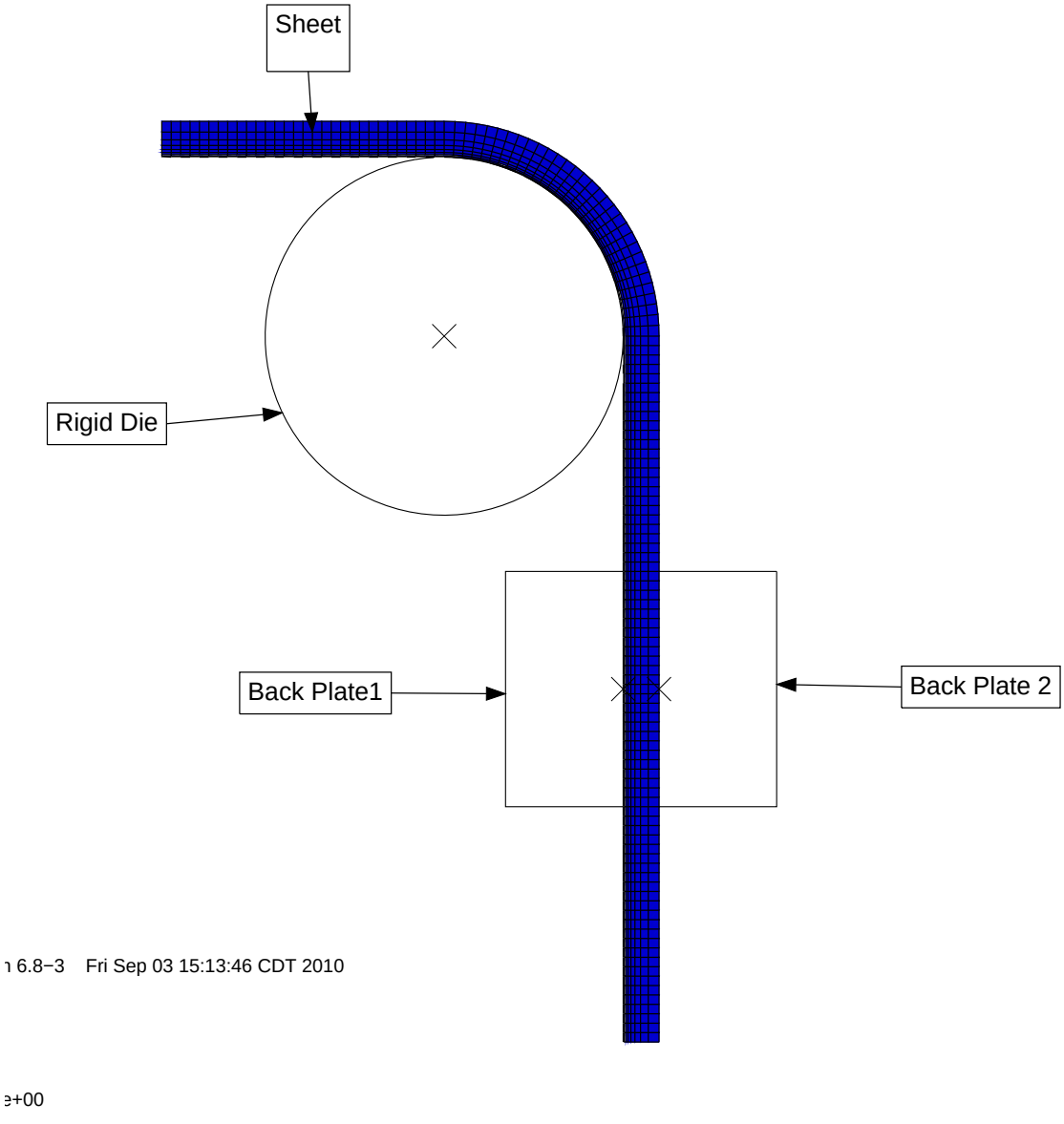

Fig. 23. Model for Numerical Simulation of Bending under Tension Test

Table XV. Material properties of aluminum substrate

Properties	Value
Material:	Aluminum 3003-H14
Density:	2.74e-09 tonnes/mm^3
Young's modulus:	63121.67
Poisson's Ratio:	0.33
Plastic Properties	
True Yield Stress(MPa)	True Plastic Strain
120.245	0
131.374	0.000343059
141.191	0.000847413
147.506	0.001392725
150.994	0.001954606
151.698	0.002850532
153.557	0.003695142
154.774	0.004562514
155.420	0.005520993
156.250	0.006716728
156.973	0.007776108
157.433	0.008810602
157.566	0.00925541

Table XVI. Material properties for PVDF coating

Properties	Value
Material:	Polyvinylidene flouride(PVDF)
Density:	1.70E-09 tonnes/mm^3
Young's Modulus:	1103.161454
Poisson Ratio:	0.3
Plastic Properties:	
True Yield Stress(MPa)	True Plastic Strain
42.1	0
46.5	0.025
47.5	0.05
47.85	0.075
47.9	0.1
47.95	0.125
47.98	0.13

D. Contact Conditions

The contact between rigid die and the sheet is defined using surface-to-surface contact method in explicit analysis. Kinematic contact method is used to enforce mechanical contact constraints which strictly allows no penetration. Finite sliding formulation is used which is more general and allows any arbitrary motion of the surfaces. The friction values obtained from experimental results between die and the sheet and between die and the back plates are used as input for the numerical simulations. Friction coefficient of 0.244 *(for r/t=5)* is applied between rigid die and the sheet with hard contact pressure over closure relationship and allowing separation after contact. Friction coefficient of 0.089 is applied between each of the back plates and the sheet with same hard contact pressure over closure relationship and allowing separation after contact.

E. Loading

In ABAQUS explicit analysis, load is applied on the sheet through back plates similar to the real experiment set up. Load of 20.65N is applied on the sheet through back plates. Displacement of the sheet through BOUNDARY type loading condition with AMPLITUDE option is given. Displacement of 12mm is applied to be ramped up in total time period of 0.2 sec. This boundary condition simulates sliding of the sheet over the die radius with a specific velocity and contact conditions.

F. Results and Discussions

Analysis were conducted for *r/t=5* and *r/t=3*. The results will be discussed for these two cases separately.

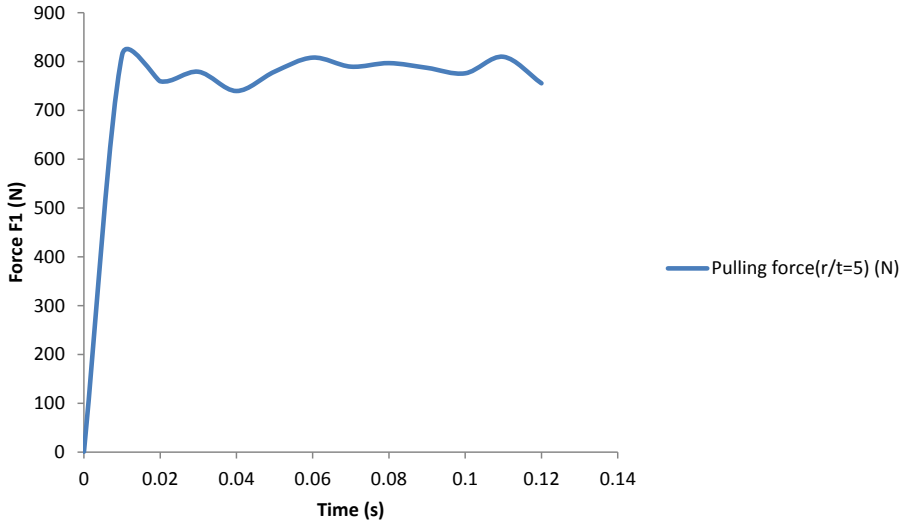

Fig. 24. Pulling Force over r/t=5

1. Die to Thickness Ratio of(r/t=5)

The sheet was drawn over r/t=5 under dry lubrication condition. The reaction forces at the pulling end of the sheet is given in Fig. 24. The trend in the pulling force recorded by FEA is same as that of experimental results as shown in Fig. 12. Higher estimation of forces in case of simulations are observed. Differences in FEA model and experiments can cause such variations in force.

One of the layers was selected from the sheet and the strain calculations were conducted along longitudinal(drawing direction) and transverse directions (thickness direction), similar to the calculations conducted for experiments. The Fig. 25(a) shows the sheet layer considered for strain calculations before drawing, the arrow in the figure shows the drawing direction. Fig. 25(b) shows the sheet layer after drawing over the radius r/t=5.

The Table. XVII shows the strain values obtained after drawing over r/t=5 radius of the die.

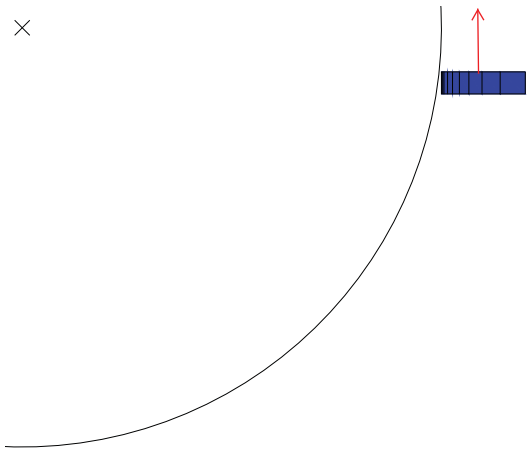

(a) Sheet layer before drawing

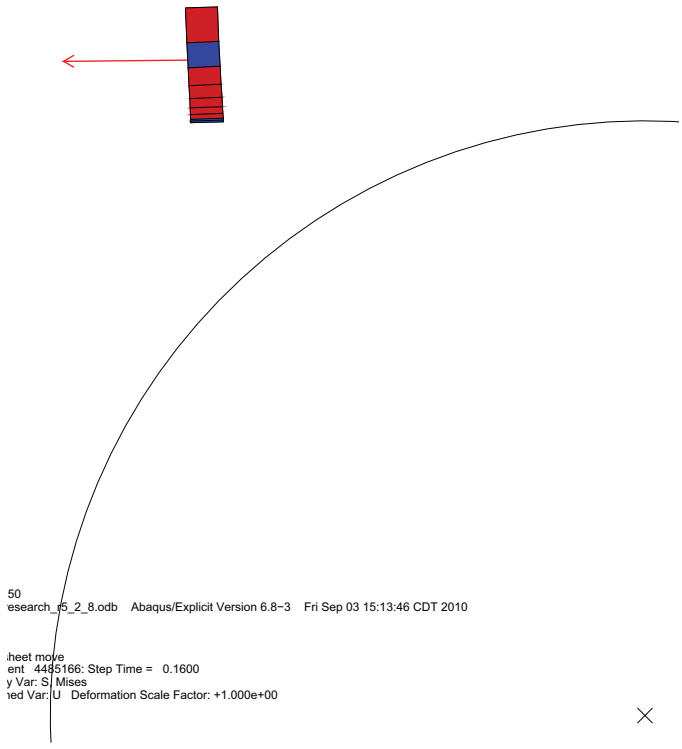

(b) Sheet layer after drawing

Fig. 25. Sheet Layer Considered for Strain Calculations

Table XVII. Strain values for r/t=5

Test	$\epsilon_{longitudinal}$	$\epsilon_{transverse}$
Numerical Simulations	3.418	-3.380
Experimental results	3.679	-3.679

Strain values obtained from numerical simulations were close to the ones obtained from experimental results. Strain in longitudinal direction is same as the strain observed in transverse direction. As strain values matches from experiments and numerical simulations , they can be used as a criteria in simulations to predict the performance of polymer coated sheet.

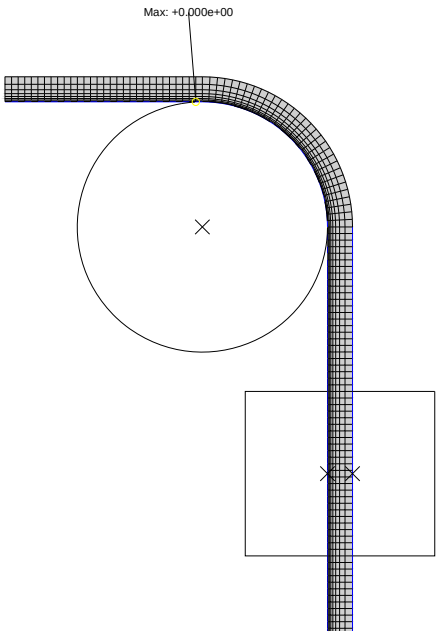

Fig. 26. Before Drawing

Another interesting observation of contact pressure was made in the simulations. A maximum contact pressure was obtained at the beginning of the drawing edge which

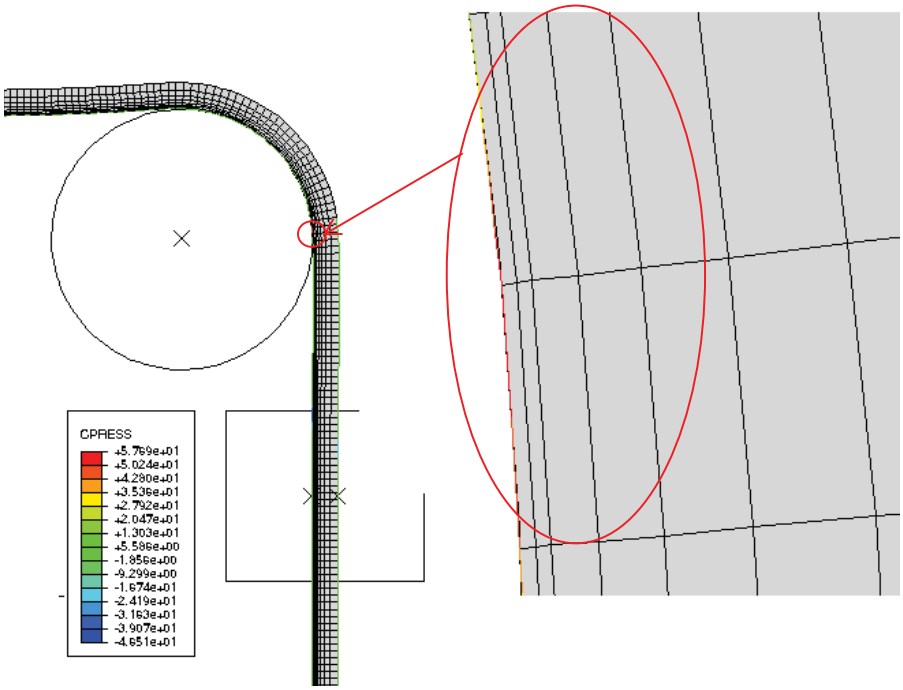

Fig. 27. Maximum Contact Pressure at the Start of Drawing

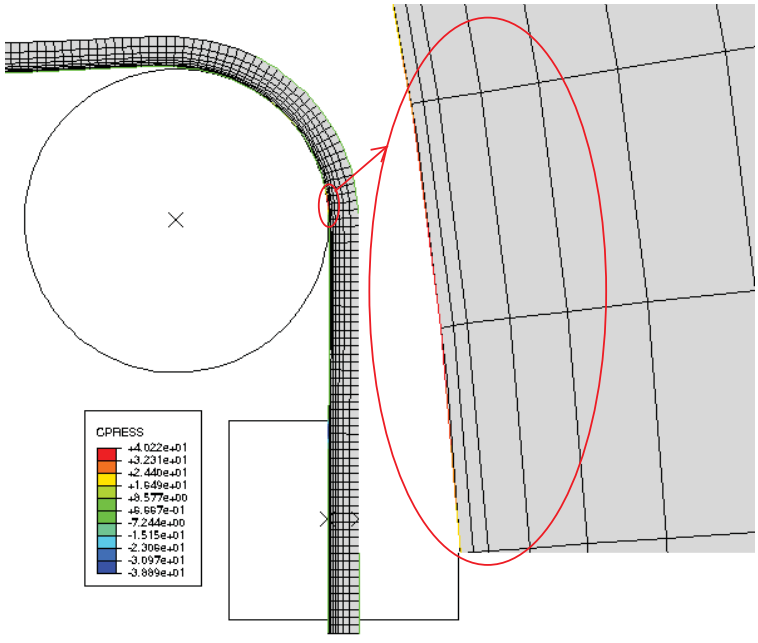

Fig. 28. Maximum Contact Pressure at 0.08 sec of 0.2 sec Drawing

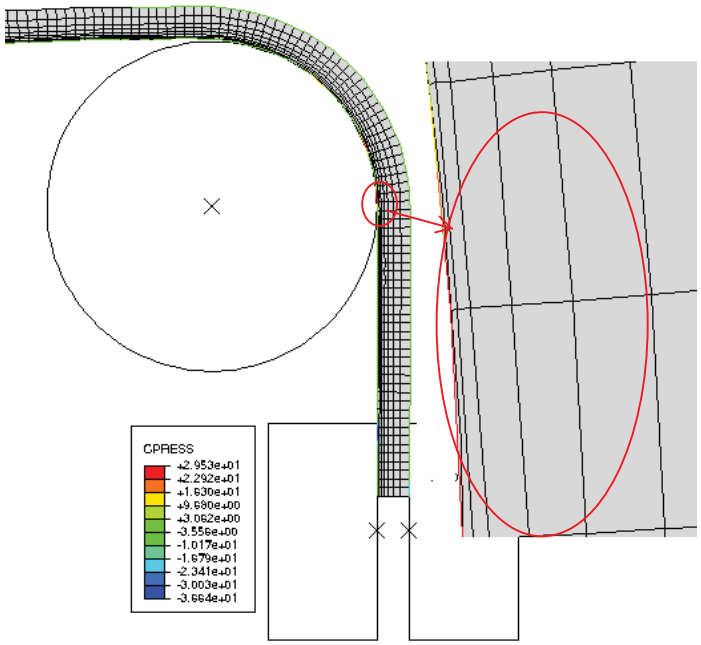

Fig. 29. Maximum Contact Pressure at 1.4 sec of 0.2 sec Drawing

is similar to the observation made by the research performed in Germany on the wear behavior of sheet metal forming tools [34]. Fig. 26 shows zero contact pressure before drawing, Fig. 27 is at t=0.01sec of 0.2sec step time, it shows the maximum contact pressure at the beginning of the drawing edge which is highlighted. Fig. 28 is at 0.08sec of 0.2 sec total step time, Fig. 29 is at 0.14sec of 0.2 sec of total step time. Both Fig. 28 and Fig. 29 shows that contact pressure is being consistently maximum at the position where drawing edge starts. Thus, the start of the drawing edge is the critical part to be studied which can effect the polymer coating.

The graph shown in Fig. 31 shows the nodal contact pressure with time. The peak value of nodal contact pressure is recorded in both the nodes when the node is at the beginning of the drawing edge.

von Mises stress distribution in the coating is shown in Fig. 30. The maximum

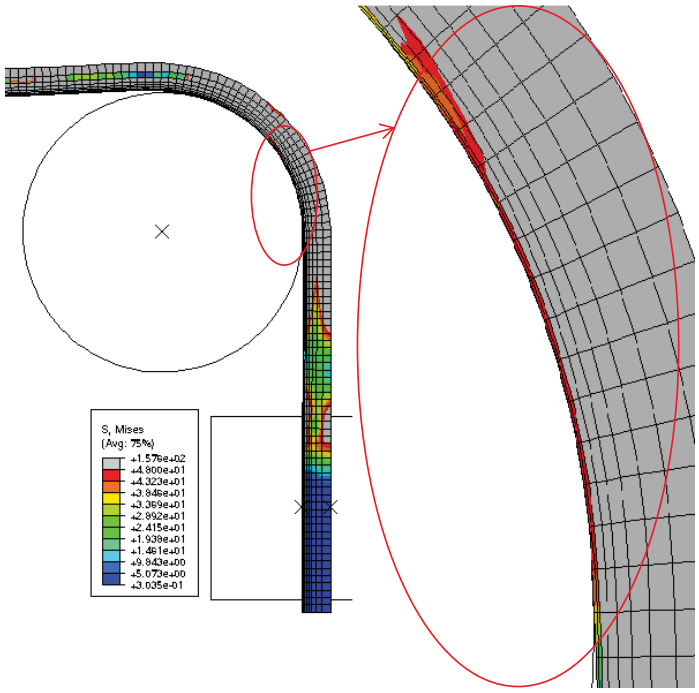

Fig. 30. von Mises Stress Distribution in Polymer Coating

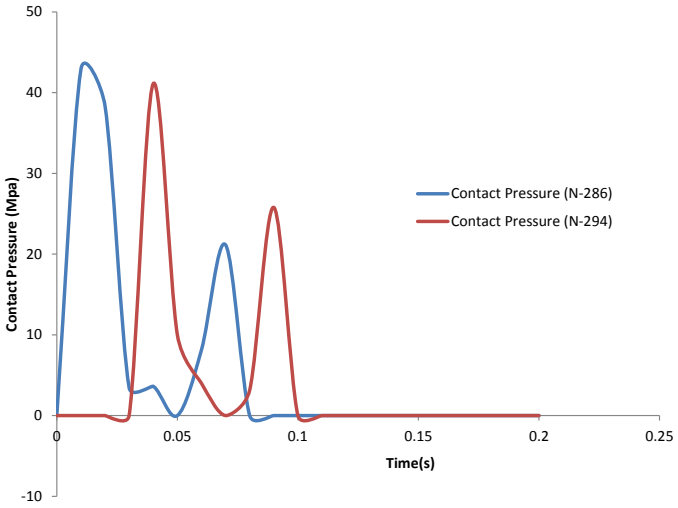

Fig. 31. Contact Pressure Variation of Nodes at Different Positions on the Die

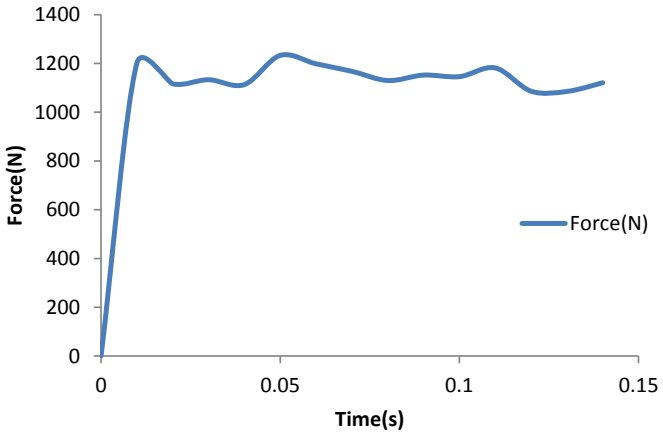

Fig. 32. Pulling Force Over r/t=3

stress is seen at the beginning of the drawing edge and at the end of the drawing edge. Maximum contact pressure at the beginning of the drawing edge is the reason for maximum stress produced in that region. Thus, numerical simulations helps in understanding the critical areas where stress in the polymer coating is high.

2. Die to Thickness Ratio of (*r/t=3*)

The force required to pull the strip around die radius of *(r/t=3)* is given in Fig.32 showing higher force required to pull around sharper die radius similar to the observation made in experiments.

Strain in longitudinal and transverse directions were calculated from simulations. Strain in longitudinal direction is 6.821% and strain in transverse direction is 6.772%. The strain for the sheets drawn over *r/t=3* is higher than the strain produced in *r/t=5* indicating more surface damage for *r/t=3* when compared to *r/t=5*.

Contact pressure was again observed to be maximum at the beginning of the drawing edge as shown in Fig. 33 which is similar to the observation made for *r/t=5*.

Apart from the location, the value of contact pressure is higher in case of r/t=3 when compared to r/t=5. This observation is very similar to the experimental observations proving that sharper radius have higher contact pressure.

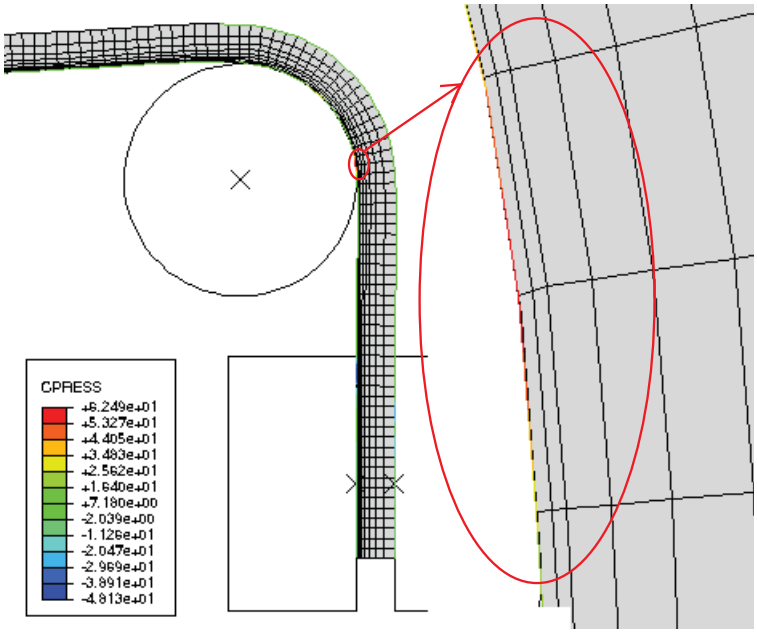

Fig. 33. Maximum Contact Pressure for r/t=3

To explain this point more clearly, the graph in Fig. 34 compares the contact pressure for *r/t=5* and *r/t=3*. Fig. 34 shows that contact pressure for *r/t=3* is higher when compared to contact pressure for *r/t=5*. With sharper radius, contact pressure increases which leads to increase in strain and more surface damage compared to less sharper die radius.

Thus, the numerical simulations showed same trend as experimental observations. Numerical simulations provided a better understanding of the contact pressure distribution and stress distribution. It provided a scope to study the influence of different die radius on the performance of polymer coating without actually conducting the experiments. Numerical simulations can also be used to study the effect of

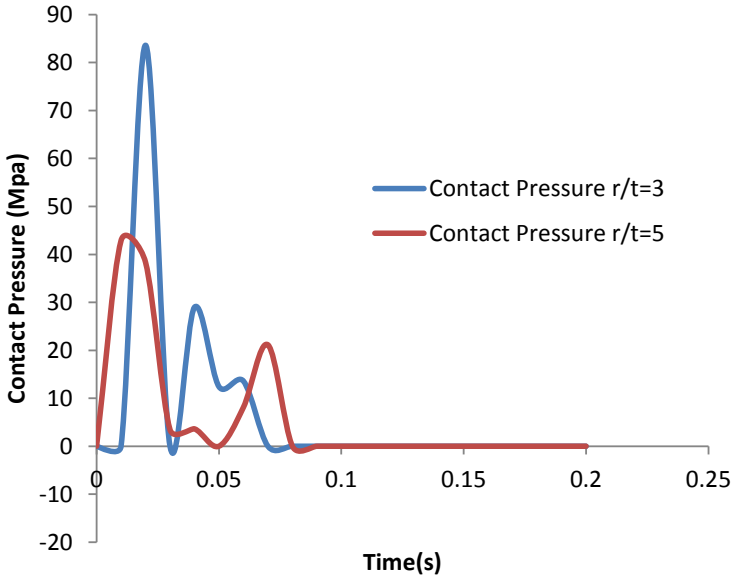

Fig. 34. Contact Pressure Comparison for r/t=3 and r/t=5

material and geometric parameters on the performance of polymer coatings.

CHAPTER VI

CONCLUSIONS AND FUTURE WORK

A. Conclusions

In the present work an experimental set-up is built to replicate the drawing of the sheet at die region of a forming process. Die assembly and fixtures are machined and integrated with electro-mechanical systems for bending under tension test set-up. Experiments are performed on polymer coated metal sheets to study coating performance under different forming conditions. Experiments are followed by numerical simulations using Finite Element Analysis package ABAQUS. The summary and conclusions from experiments and numerical simulations are summarized below.

1. Bending under tension test can give an accurate prediction for the performance of polymer coatings, as it closely simulates the real forming process. Bending of the sheet, being an important parameter, is considered in this set-up and in friction calculations.

2. Die radius has a major effect on the surface quality of polymer coatings. With decrease in die radius, contact pressure between die and sheet increases which leads to higher friction and surface damage. The value of coefficient of friction measured for *r/t=5* die radius was higher than *r/t=10* die radius.

3. Lubricating conditions also have an impact on polymer coatings. Three lubricating conditions; dry, diluted and pure are studied. Pure lubrication condition has lowest COF and good surface appearance. COF for diluted lubricant increases during the test because it is less viscous in nature and is squeezed out gradually. For dry lubrication, COF and surface damage is highest compared

to other two conditions as expected.

4. Though lubrication has some effect on the COF, the influence is not as significant as that of die radius. This is attributed to the fact that the polymer coating itself acts as a solid lubricant in the test. Therefore, there is not much difference seen on using additional lubricant.

5. Effect of material is also studied by conducting experiments on Material1 (PVDF coated metal sheets) and Material4 (Polypropylene coated metal sheets). Polypropylene being the softer material as compared to PVDF coating, is observed to have more scratches on the surface. Along with comparing materials with different properties, materials with different surface topography are also compared. Material with textured surface topography shows higher damage as compared to material with non-textured one.

6. The hardness of the polymer coating studied using nano indentation test, shows lower hardness for sharper die radius. This indicates softening of the polymer.

7. Strain calculations showed increase in strain when drawn over sharper die radius. Strain in drawing direction is lowest for *r/t=10* radius followed by *r/t=5* radius and highest for *r/t=1* radius. Strain calculations are used to compare results from experiments and numerical simulations.

8. FEA simulations are conducted for different die radii. The values obtained for strain and pulling force are comparable to the one from experiments.

9. Maximum contact pressure and von Mises stress are concentrated at the beginning of the drawing edge. Value of maximum contact pressure for *r/t=3* die radius is higher than *r/t=5* die radius as measured from FEA simulations.

Thus, for smaller die radius, contact pressure is higher and therefore COF is higher which supports the experiment results. Numerical simulations help in understanding the critical areas where stresses are high.

To conclude, bending under tension test gives an accurate way to evaluate the performance of polymer coatings, as it considers both friction and bending effects. Effect of die radius is more critical than lubrication; higher contact pressure and stresses are concentrated at the beginning of the drawing edge. Numerical simulations provide a means to vary material and geometric parameters independently to study their effects on the performance of polymer coatings.

B. Future Work

Although the critical area which affects the performance of polymer coatings is die region where the sheet bends and unbends, investigating the effect of varying COF at the back plates is also recommended.

Use of better surface imaging techniques such as scanning electron microscope is required to get better understanding of the wear mechanism on the surface of the polymer coatings.

The present study can be extended by considering effect of variables such as strain rate and angle of contact on the performance of polymer coatings.

A test set-up which is more automated can be designed and manufactured for ease of use.

Numerical simulations can be used to study the effect of material properties and detailed study of the stress distribution in the polymer coatings.

REFERENCES

[1] National Coil Coating Association, Cleveland, Ohio, *Coil Coating, Technical Bulletin*, June 1996.

[2] W.D. Callister, *Materials science and engineering: an introduction*, chapter Polymer Structures, pp. 460–488, John Wiley & Sons, Inc., New York, NY, 2007.

[3] United States Steel Corporation, Fairfield, Alabama, *Paint Systems Used in The Construction Market, Technical Bulletin*, October 2005.

[4] M.P. Groover, *Fundamentals of Modern Manufacturing: Materials, Processes, and Systems*, John Wiley & Sons, New York, NY, 2004.

[5] M.J. van den Bosch, P.J.G. Schreurs, and M.G.D. Geers, "Identification and characterization of delamination in polymer coated metal sheet," *Journal of the Mechanics and Physics of Solids*, vol. 56, no. 11, pp. 3259–3276, 2008.

[6] S. GmbH, *Metal Forming Handbook*, vol. 1, Springer Verlag, Berlin, New York, 1^{st} edition, 1998.

[7] I.M. Hutchings and E. Arnold, *Tribology: Friction and Wear of Engineering Materials*, vol. 1, Elsevier Limited, London, UK, 16^{th} edition, 1992.

[8] G.W. Stachowiak, A.W. Batchelor, and G.W. Stachowiak, *Engineering Tribology*, vol. 1, Butterworth-Heinemann, Boston, MA, 3^{rd} edition, 2001.

[9] P. Carlsson, "Surface engineering in sheet metal forming," Ph.D. dissertation, Acta Universitatis Upsaliensis Uppsala, Uppsala, Sweden, 2005.

[10] D.W. Vallance and O.K. Matlock, "Application of the bending-under-tension friction test to coated sheet steels," *Journal of Materials Engineering and Performance*, vol. 1, pp. 685–693, October 1992.

[11] P. Viorel and N. Dumitru, "Simulation of friction phenomenon in deep drawing process," *ANNALS*, vol. 24, pp. 26, 2003.

[12] D. Schmoeckel, H. Frontzek, and E. von Finckenstein, "Reduction of wear on sheet metal forming tools," *CIRP Annals-Manufacturing Technology*, vol. 35, pp. 195–198.

[13] H.W. Swift, "Plastic bending under tension," *Engineering*, vol. 166, pp. 333–359, 1948.

[14] R.T. Fox, A.M. Maniatty, and D. Lee, "Determination of friction coefficient for sheet materials under stretch-forming conditions," *Metallurgical and Materials Transactions A*, vol. 20, no. 10, pp. 2179–2182, 1989.

[15] M. Sulonen, P. Eskola, J. Kumpulainen, and A. Ranta-Eskola, "A reliable method for measuring the friction coefficient in sheet metal forming," in *Proceedings of IDDRG WG-Meeting*, Japan, January 1981, IDDRG WG, Paper WG III/4.

[16] W.R.D. Wilson, H.G. Malkani, and P.K. Saha, "Boundary friction measurements using a new sheet metal forming simulator," *Trans. NAMRI/SME*, pp. 37–42, 1991.

[17] P.K. Saha, "Boundary friction measurements in sheet metal forming," Ph.D. dissertation, University Microfilms International, Ann Arbor, MI, 1993.

[18] A. Azushima and M. Sakuramoto, "Effects of plastic strain on surface roughness and coefficient of friction in tension-bending test," *CIRP Annals-Manufacturing Technology*, vol. 55, no. 1, pp. 303–306, 2006.

[19] ZHANG Wei-gang HOU Ying-Ke, YU Zhang-qi, "Surface topography evolvement of galvanized steels in sheet metal forming," *Transactions of Nonferrous Metals Society of China*, vol. 19, no. 2, pp. 305 – 310, 2009.

[20] L. Fratini, S. Lo Casto, and E. Lo Valvo, "A technical note on an experimental device to measure friction coefficient in sheet metal forming," *Journal of Materials Processing Technology*, vol. 172, no. 1, pp. 16–21, 2006.

[21] I. Manika and J. Maniks, "Effect of substrate hardness and film structure on indentation depth criteria for film hardness testing," *Journal of Physics D: Applied Physics*, vol. 41, pp. 1–6, 2008.

[22] W. Shen, B. Jiang, S.M. Gasworth, and H. Mukamal, "Study of tribological properties of coating/substrate system in micrometer and nanometer scales with a scanning probe microscope," *Tribology International*, vol. 34, no. 2, pp. 135–142, 2001.

[23] N. Panich, P. Wangyao, T. Chomtohsuwan, and S. Yong, "Finite element analysis of the critical ratio of coating thickness to indentation depth of soft coating on a harder substrate by nanoindentation," *ScienceAsia*, vol. 32, pp. 411–416, 2006.

[24] J.S.S. Wong, H.J. Sue, K.Y. Zeng, R.K.Y. Li, and Y.W. Mai, "Scratch damage of polymers in nanoscale," *Acta Materialia*, vol. 52, no. 2, pp. 431–443, 2004.

[25] M. Wong, G.T. Lim, A. Moyse, J.N. Reddy, and H.J. Sue, "A new test methodology for evaluating scratch resistance of polymers," *Wear*, vol. 256, no. 11-12, pp. 1214–1227, 2004.

[26] G.T. Lim, M.H. Wong, J.N. Reddy, and H.J. Sue, "An integrated approach towards the study of scratch damage of polymer," *Journal of Coatings Technology and Research*, vol. 2, no. 5, pp. 361–369, 2005.

[27] R.L. Browning, G.T. Lim, A. Moyse, H.J. Sue, H. Chen, and J.D. Earls, "Quantitative evaluation of scratch resistance of polymeric coatings based on a standardized progressive load scratch test," *Surface and Coatings Technology*, vol. 201, no. 6, pp. 2970–2976, 2006.

[28] R.L. Browning, H. Jiang, and H.J. Sue, "Scratch behavior of polymeric materials," *Tribology and Interface Engineering Series*, vol. 55, pp. 354–373, 2008.

[29] P. Carlsson, U. Bexell, and M. Olsson, "Friction and wear mechanisms of thin organic permanent coatings deposited on hot-dip coated steel," *Wear*, vol. 247, no. 1, pp. 88–99, 2001.

[30] P. Carlsson, U. Bexell, and M. Olsson, "Tribological behaviour of thin organic permanent coatings deposited on hot-dip coated steel sheet–a laboratory study," *Surface and Coatings Technology*, vol. 132, no. 2-3, pp. 169–180, 2000.

[31] P. Carlsson, U. Bexell, and M. Olsson, "Tribological performance of thin organic permanent coatings deposited on 55% al-zn coated steel–influence of coating composition and thickness on friction and wear," *Wear*, vol. 251, no. 1-12, pp. 1075–1084, 2001.

[32] Hysitron Inc., Minneapolis, MN, *Tribo Indenter Users Manual*, July 2001.

[33] T. Koch and S. Seidler, "Correlations between indentation hardness and yield stress in thermoplastic polymers," *Strain*, vol. 45, no. 1, pp. 26–33, 2009.

[34] C. Muller P. Groche, M. Engels, "Wear behavior of sheet metal forming tools made from nodular cast iron after mechanical surface treatments," *Transactions of NAMRI/SME*, vol. 38, no. 1, pp. 531–538, 2010.

APPENDIX A

ENGINEERING DRAWINGS OF DIE ASSEMBLY

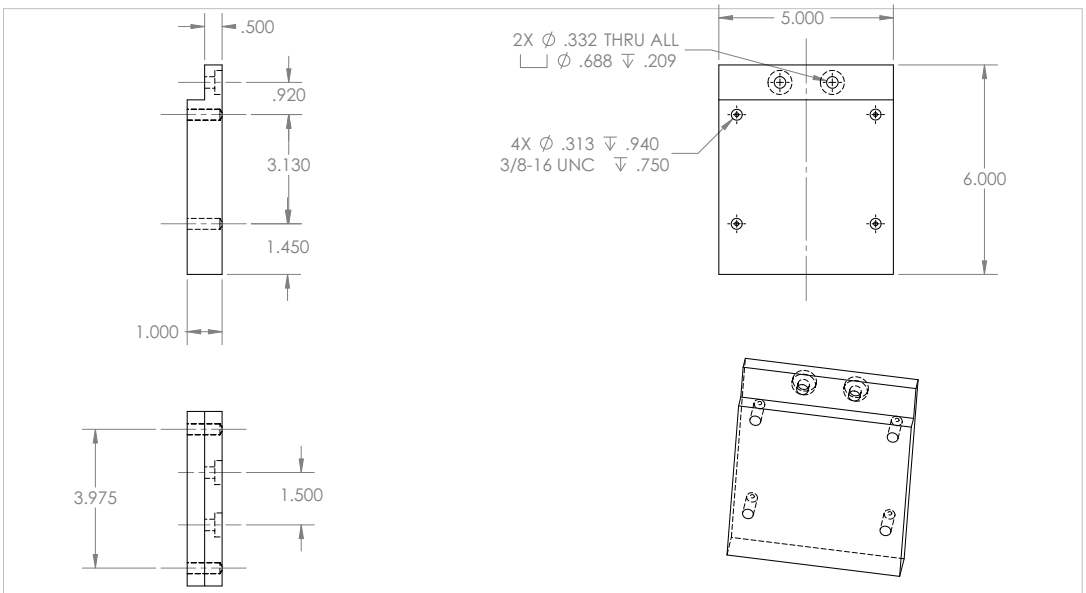

UNLESS OTHERWISE SPECIFIED:		NAME	DATE
DIMENSIONS ARE IN INCHES TOLERANCES: FRACTIONAL ± ANGULAR: MACH ± BEND ± TWO PLACE DECIMAL ± THREE PLACE DECIMAL ±	DRAWN	ZP	6/2/2010
	CHECKED		
	ENG APPR.		
	MFG APPR.		
INTERPRET GEOMETRIC TOLERANCING PER:	Q.A.		
MATERIAL: 4140 Steel	COMMENTS: Quantity 1		
FINISH			
DO NOT SCALE DRAWING			

Texas A&M University

TITLE: Die Holder

SIZE	DWG. NO.	REV
A	Part1	

SCALE: 1:3 | WEIGHT: | SHEET 1 OF 1

4 3 2 1

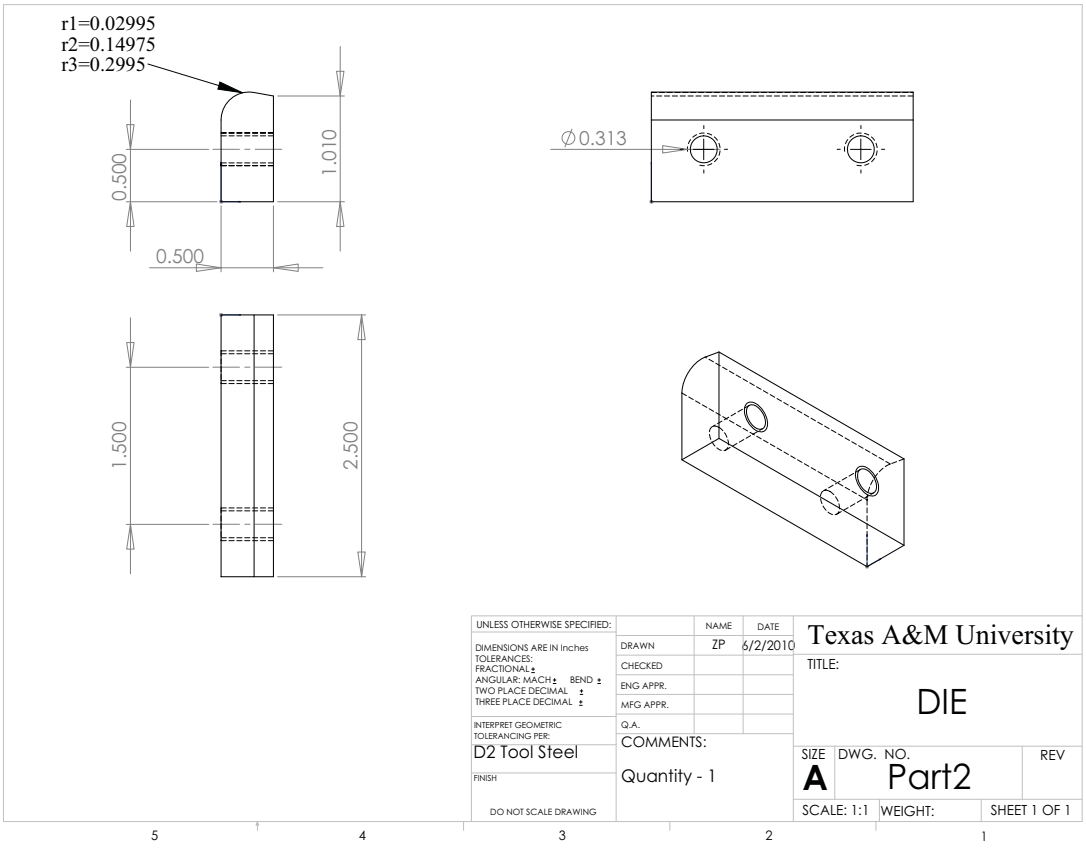
r1=0.02995
r2=0.14975
r3=0.2995
0.500
1.010
0.500
∅0.313
1.500
2.500
UNLESS OTHERWISE SPECIFIED:
DIMENSIONS ARE IN Inches
TOLERANCES:
FRACTIONAL ±
ANGULAR: MACH ± BEND ±
TWO PLACE DECIMAL ±
THREE PLACE DECIMAL ±
INTERPRET GEOMETRIC TOLERANCING PER:
D2 Tool Steel
FINISH
DO NOT SCALE DRAWING
NAME
DATE
DRAWN
ZP
6/2/2010
CHECKED
ENG APPR.
MFG APPR.
Q.A.
COMMENTS:
Quantity - 1
Texas A&M University
TITLE:
DIE
SIZE
A
DWG. NO.
Part2
REV
SCALE: 1:1
WEIGHT:
SHEET 1 OF 1
5
4
3
2
1

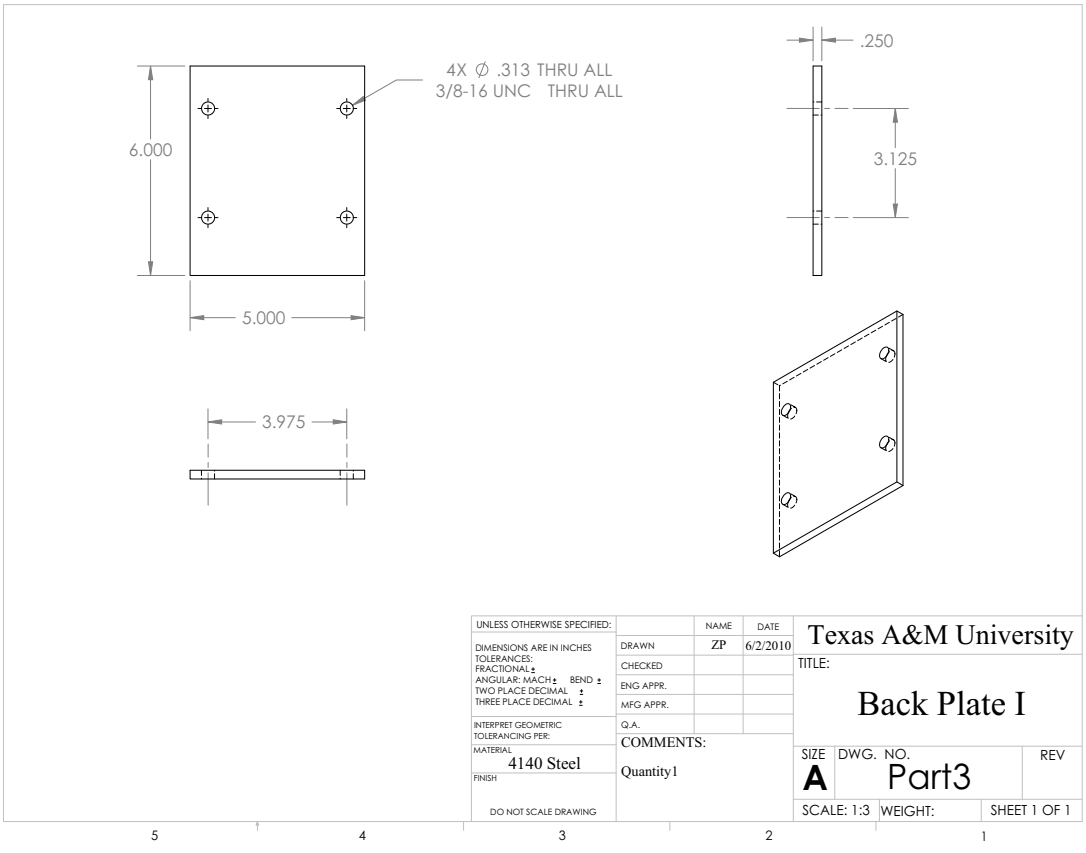

UNLESS OTHERWISE SPECIFIED:		NAME	DATE
DIMENSIONS ARE IN INCHES TOLERANCES: FRACTIONAL ± ANGULAR: MACH ± BEND ± TWO PLACE DECIMAL ± THREE PLACE DECIMAL ±	DRAWN	ZP	6/2/2010
	CHECKED		
	ENG APPR.		
	MFG APPR.		
INTERPRET GEOMETRIC TOLERANCING PER:	Q.A.		
MATERIAL: 4140 Steel	COMMENTS: Quantity1		
FINISH			
DO NOT SCALE DRAWING			

Texas A&M University		
TITLE: Back Plate I		
SIZE: A	DWG. NO.: Part3	REV
SCALE: 1:3	WEIGHT:	SHEET 1 OF 1

5 4 3 2 1

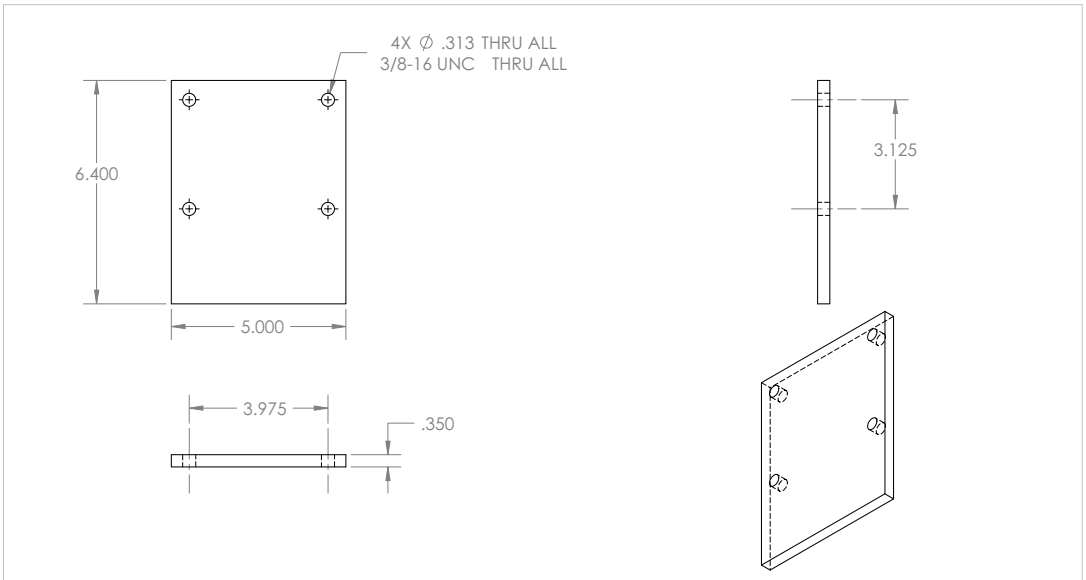

UNLESS OTHERWISE SPECIFIED:		NAME	DATE
DIMENSIONS ARE IN INCHES TOLERANCES: FRACTIONAL ± ANGULAR: MACH ± BEND ± TWO PLACE DECIMAL ± THREE PLACE DECIMAL ±	DRAWN	ZP	7/15/2010
	CHECKED		
	ENG APPR.		
	MFG APPR.		
INTERPRET GEOMETRIC TOLERANCING PER:	Q.A.		
MATERIAL: Aluminum	COMMENTS: Quantity1		
FINISH			
DO NOT SCALE DRAWING			

Texas A&M University

TITLE: Back Plate II

SIZE	DWG. NO.	REV
A	Part4	

SCALE: 1:3	WEIGHT:	SHEET 1 OF 1

5 4 3 2 1

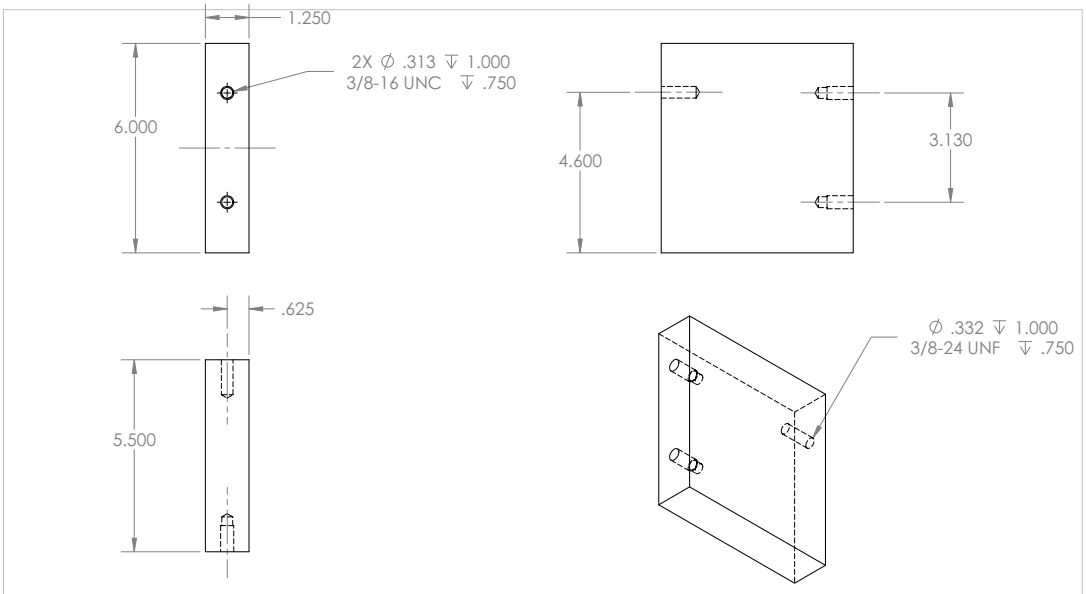

UNLESS OTHERWISE SPECIFIED:		NAME	DATE
DIMENSIONS ARE IN INCHES TOLERANCES: FRACTIONAL ± ANGULAR: MACH ± BEND ± TWO PLACE DECIMAL ± THREE PLACE DECIMAL ±	DRAWN	ZP	15/7/2010
	CHECKED		
	ENG APPR.		
	MFG APPR.		
INTERPRET GEOMETRIC TOLERANCING PER:	Q.A.		
MATERIAL: Aluminum	COMMENTS: Quantity 2		
FINISH			
DO NOT SCALE DRAWING			

Texas A&M University		
TITLE: Vertical Plates		
SIZE: A	DWG. NO.: part5	REV
SCALE: 1:3	WEIGHT:	SHEET 1 OF 1

5 4 3 2 1

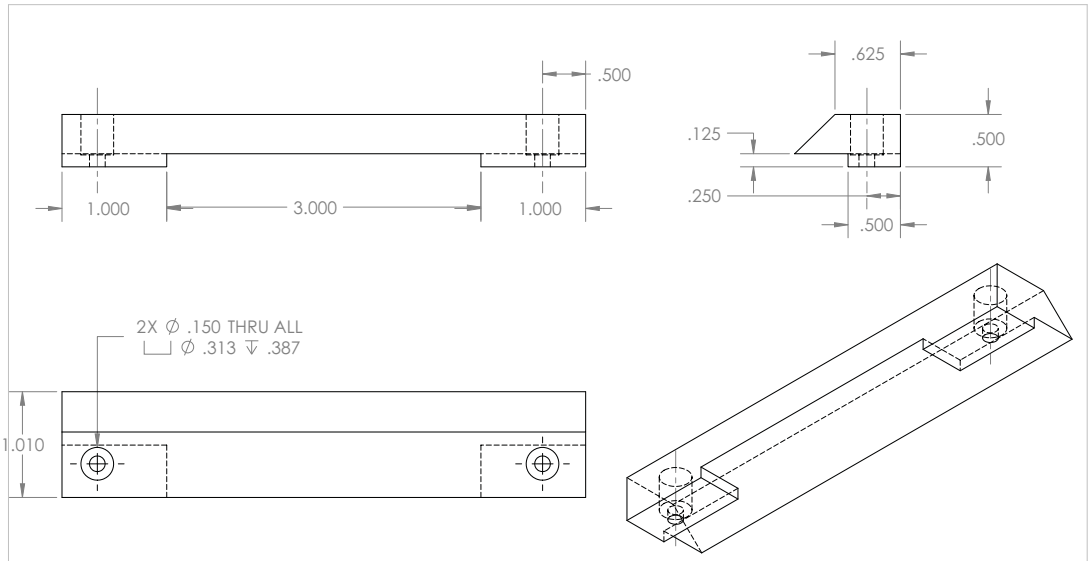

UNLESS OTHERWISE SPECIFIED:		NAME	DATE
DIMENSIONS ARE IN INCHES TOLERANCES: FRACTIONAL ± ANGULAR: MACH ± BEND ± TWO PLACE DECIMAL ± THREE PLACE DECIMAL ±	DRAWN	ZP	
	CHECKED		
	ENG APPR.		
	MFG APPR.		
INTERPRET GEOMETRIC TOLERANCING PER:	Q.A.		
MATERIAL: 4140 Steel	COMMENTS: Quantity1		
FINISH			
DO NOT SCALE DRAWING			

Texas A&M University		
TITLE: Top Support Plate		
SIZE: A	DWG. NO.: part6	REV
SCALE: 1:1	WEIGHT:	SHEET 1 OF 1

5 4 3 2 1

APPENDIX B

DATA SHEET SHOWING DATA OBTAINED FROM LOAD SENSORS AND CALCULATIONS FOR COEFFICIENT OF FRICTION AT DIE REGION

Table XVIII. Calculations of bending force F_b for Material1

Die Radius	Yield Strength($\sigma_y inN/mm^2$)	Thickness (t in mm)	Width (W in mm)	Radius of Curvature (r in mm)	Bending force ($F_b = \frac{\sigma_y * st^2 * W}{2*r} inN$)
r10(r/t=10)	151	0.7613	36.322	7.988	198.682
r5(r/t=5)	151	0.7613	36.322	4.184	379.301

Table XIX. Data obtained from load sensors for Material1 under dry condition and r/t=5

Time(sec)	Load Cell I(F1 in N)	Load Cell II(N in N)	COF at back plate(μ_b)	F2($F2 = \mu_b * N$ in N)
1	642.24	673.27	0.178	119.84206
2	646.63	674.67	0.178	120.091
3	634.9	675.87	0.178	120.305
4	635.5	676	0.178	120.328
5	632.43	674.5	0.178	120.061
6	623.58	674.26	0.178	120.018
7	635.61	673.05	0.178	119.803
8	620.03	671.83	0.178	119.586
9	634.97	671.83	0.178	119.586
10	638.57	673.29	0.178	119.846
11	635.82	672.94	0.178	119.783
12	630.96	671.9	0.178	119.599
13	593.17	670.92	0.178	119.424
14	603.47	670.47	0.178	119.344
15	593.6	675.2	0.178	120.185
16	616.31	673.11	0.178	119.814
17	622.01	671.79	0.178	119.579
18	631.59	673.58	0.178	119.897
19	615.78	667.71	0.178	118.852
20	623.3	663.32	0.178	118.071

Table XX. COF calculations for Material1 under dry condition and r/t=5

F1(N)	F2(N)	F_b(N)	θ(radians)	COF at die region ($\mu_d = (\frac{2}{\theta})(\frac{F1-F2-F_b}{F1+F2})$)
642.24	119.84206	379.301	1.57	0.284631229
646.63	120.091	379.301	1.57	0.290
634.9	120.305	379.301	1.57	0.274
635.5	120.328	379.301	1.57	0.275
632.43	120.061	379.301	1.57	0.272
623.58	120.018	379.301	1.57	0.261
635.61	119.803	379.301	1.57	0.276
620.03	119.586	379.301	1.57	0.257
634.97	119.586	379.301	1.57	0.276
638.57	119.846	379.301	1.57	0.280
635.82	119.783	379.301	1.57	0.277
630.96	119.599	379.301	1.57	0.271
593.17	119.424	379.301	1.57	0.220
603.47	119.344	379.301	1.57	0.235
593.6	120.185	379.301	1.57	0.220
616.31	119.814	379.301	1.57	0.251
622.01	119.579	379.301	1.57	0.259
631.59	119.897	379.301	1.57	0.271
615.78	118.852	379.301	1.57	0.253
623.3	118.071	379.301	1.57	0.264

VITA

Name: Zalak Purohit

Address: Department of Mechanical Engineering, Texas A&M University,
Mail stop 3123 College Station, Texas 77843.

Email Id: pzalak@neo.tamu.edu

Education: B.E., Mechanical Engineering, Chaitanya Bharathi Institute of Technology, Osmania University, India, 2008

M.S., Mechanical Engineering, Texas A&M University,
College Station, Texas, 2010

The typist for this thesis was Zalak purohit.